Cenozoic volcanism in the Sierra Nevada and Walker Lane, California, and a new model for lithosphere degradation

Keith Putirka[1,*], Marlon Jean[2,*], Brian Cousens[3,*], Rohit Sharma[1,*], Gerardo Torrez[1,*], and Chad Carlson[1,*]
[1]*Department of Earth and Environmental Sciences, California State University, 2576 E. San Ramon Avenue, MS/ST24, Fresno, California 93740-8039, USA*
[2]*Department of Geology, Utah State University, 4505 Old Main Hill, Logan, Utah 84322, USA*
[3]*Department of Earth Sciences, Carleton University, 1125 Colonel By Drive, Ottawa, Ontario K1S 5B6, Canada*

ABSTRACT

Volcanic rock and mantle xenolith compositions in the Sierra Nevada (western United States) contradict a commonly held view that continental crust directly overlies asthenosphere beneath the Sierran range front, and that ancient continental mantle lithosphere (CML) was entirely removed in the Pliocene. Instead, space-time trends show that the Walker Lane is the principle region of mantle upwelling and lithosphere removal in eastern California, that lithosphere loss follows the migration of the Mendocino Triple Junction (MTJ), and that the processes of lithosphere removal are not yet complete beneath the Sierra Nevada and its range front. Key evidence is provided by volcanic rock compositions. The $^{87}Sr/^{86}Sr$ ratios for mafic volcanics of the Sierra (MgO > 8%) are mostly > 0.705, and $^{143}Nd/^{144}Nd$ < 0.5127, much unlike eastern sub-Pacific asthenosphere (where $^{87}Sr/^{86}Sr$ < 0.7027 and $^{143}Nd/^{144}Nd$ > 0.5129), but very much like CML. Similarly, Sierran volcanics carry CML-like trace element ratios, with La/Nb > 3 and Th/Nb > 1, values that are significantly higher than asthenosphere-derived melts (La/Nb < 1.5, Th/Nb < 0.08). Spinel-bearing mantle xenoliths contained in Pleistocene–Holocene volcanics from the Sierran range front also have a CML composition, with $^{87}Sr/^{86}Sr$ and ε_{Nd} ratios that range to 0.7065 and –3.6, respectively. New estimates of melt extraction depths using Si activity and mineralogy-sensitive trace element ratios (Sm/Yb, Lu/Hf) show that CML extends from the base of the crust (40 km) to depths of 75 km beneath the range front, and to 110 km for Pliocene volcanics of the southern Sierra. This means that garnet-bearing lithologies could not have been dislodged from beneath the southern Sierra until after the Pliocene. Only in the Walker Lane do young (0.18 Ma) volcanic rocks, from the Coso volcanic field, approach asthenosphere-like compositions, which occurs only 20 Ma after MTJ arrival. Temporal trends show that MTJ arrival at any given latitude south of 37°N signals lithosphere heating, probably due to asthenosphere that upwells to replace the sinking Farallon plate. Partial melts of the asthenosphere, and perhaps the asthenosphere itself, intrude into and cause heating and partial melting of overlying CML; this culminates after 10 Ma. After 20 Ma, CML becomes highly degraded and asthenosphere-derived melts are dominant. North of 37°N, volcanic rocks approach asthenosphere-derived compositions to the west, not the east, and $^{87}Sr/^{86}Sr$ ratios increase from 18 to 0 Ma, indicating that this region has entered a phase of lithosphere heating, but not yet a phase of lithosphere removal.

We propose a new model of lithosphere degradation, where asthenosphere or its partial melts pervasively invade CML beneath the Walker Lane. This process is now nearly complete beneath Coso, and is migrating west, so that it is only partly complete at the southern Sierra range front, or within the Sierra Nevada, at any latitude. This model of intermixed asthenosphere and lithosphere better explains the compositions of volcanic rocks and their included xenoliths, and the remarkably consistent S-wave receiver function data, which show a 70-km-thick lithosphere beneath the Sierra Nevada. If the upper mantle is warm CML, permeated by partial melts, this model may also explain low P- and S-wave velocities.

*Emails: Putirka: kputirka@csufresno.edu; Jean: m.m.j@aggiemail.usu.edu; Cousens: bcousens@earthsci.carleton.ca; Sharma: rohits@mail.fresnostate.edu; Torrez: gtorrez2@mail.fresnostate.edu; Carlson: ameanchad@hotmail.com.

INTRODUCTION

There is a fundamental conflict in our understanding of basaltic volcanism in and adjacent to the Sierra Nevada and in some seismology-based interpretations of underlying mantle. Geochemical studies clearly show that Miocene to Holocene volcanism in the Sierra Nevada (western United States), at least from the Lake Tahoe region southward, requires partial melting of an enriched continental mantle lithosphere (CML) source (e.g., Leeman, 1974; Beard and Glazner, 1995; Cousens, 1996; Lee, 2005; Putirka and Busby, 2007; Cousens et al., 2008; Blondes et al., 2008). This is true even at the southeastern margin of the range, where it was argued (Cousens et al., 2008) that enriched mantle must be beneath the very young Big Pine, Coso, and Long Valley volcanic fields. Geochemical studies of CML thinning place maximum thinning to the east of the Sierra Nevada range front (e.g., Ormerod et al., 1988; DePaolo and Daley, 2000). However, some recent seismic data yield low P- and S-wave velocities in the uppermost mantle beneath the Sierra Nevada, data sometimes interpreted to indicate that continental crust directly overlies asthenosphere in the southern Sierra (e.g., Fliedner and Ruppert, 1996; Wernicke et al., 1996; Savage et al., 2003; Jones et al., 2004; Zandt et al., 2004), and perhaps as far north as Lake Tahoe (Frassetto et al., 2011). These seismic studies are in conflict with S-wave receiver function data indicating that the lithosphere is 70 km thick throughout the range (Li et al., 2007). These contrasting views provide an unclear view of lithosphere degradation and volcanism in the wake of Miocene–Holocene plate reorganization (e.g., Atwater and Stock, 1998). We examine the volcanic record of the Sierran mantle, and propose a new model of lithosphere degradation to rectify geochemical and seismic observations.

Geosphere; April 2012; v. 8; no. 2; p. 265–291; doi:10.1130/GES00728.1; 17 figures; 1 table; 2 supplemental tables.

TABLE 1. DATA USED IN THIS STUDY

Volcanic field	Age (Ma)	Latitude (°N)	Province	Tectonic setting*	Data sources†
Mount Shasta and Medicine Lake	0–3.6	41.2–41.9	Cascades	Pre-MTJ	Supplemental Table 2: Grove et al. (1988), Donnelly-Nolan et al. (1991), Baker et al. (1994)
Lassen	0–3.6	40.0–40.7	Cascades and/or Sierra Nevada	Pre-MTJ	Supplemental Table 2: Anderson and Gottfried (1971), Bullen and Clynne (1990), Borg and Clynne (1998)
Dixie Mountain	10–12 Ma	39.2–40.0	Cascades and/or Sierra Nevada	Pre-MTJ	Supplemental Table 1: Roullet (2006)
Lake Tahoe	1.4–16.3	39.1–39.6	Sierra Nevada and/or Ancestral Cascades	Transitional	Supplemental Table 2: Cousens et al. (2008)
Central Sierra Nevada	4.0–15.5	38.0–38.8	Sierra Nevada and/or Ancestral Cascades	Transitional	Supplemental Table 1: This study; Putirka and Busby (2007), Busby et al. (2008a, 2008b), Hagan et al. (2009), Koerner et al. (2009); Busby and Putirka (2009)
Bodie Hills	6–13.2	36.2–38.4	Basin and Range	Transitional	David John (2011, personal commun.)
Long Valley	0–3.6	37.6–37.8	Sierra Nevada and/or Basin and Range	Post-MTJ	Supplemental Table 2: Ormerod (1988), Dodge and Moore (1981), Cousens (1996), Bailey (2004)
Southern Sierra					Supplemental Table 2: Moore and Dodge (1980), Van Kooten (1980), Dodge and Moore (1981), Farmer et al. (2002), Feldstein and Lange (1999)
Miocene (MgO = 1.4%–11.8%)	8.6–12.8	35.8–37.5	Sierra Nevada	Post-MTJ	
Pliocene (MgO = 5.6%–12.1%)	2.6–3.9	35.8–37.5	Sierra Nevada	Post MTJ	
Deep Springs	2.6	37.3	Basin & Range	Post-MTJ	Supplemental Table 2: Beard and Glazner (1998)
Big Pine	0–1.3	36.9–37.1	Sierra Nevada and/or Basin and Range	Post-MTJ	Supplemental Table 2: Dodge and Moore (1981), Ormerod (1988), Ormerod et al. (1991), Beard and Glazner (1995), Waits (1995), Blondes et al. (2008)
Panamint Valley/Saline Range	2–2.4	36.8–36.9	Basin and Range	Post-MTJ	Supplemental Table 2: Hoffine (1993)
Death Valley	2–6	36.3–36.9	Basin and Range	Post-MTJ	Supplemental Table 2: Walker and Coleman (1991), Hoffine (1993)
Coso	0–8.3	35.8–36.3	Sierra Nevada and/or Basin and Range	Post MTJ	Babcock (1977), Bacon et al. (1981, 1984), MacDonald et al. (1992), Groves (1996), DePaolo and Daley (2000)

*Tectonic setting is based on Equation 1 (see text); MTJ is Mendocino Triple Junction; transitional indicates that volcanic field contains rocks erupted both pre-MTJ and post-MTJ arrival.
†For Supplemental Tables 1 and 2, see footnotes 1 and 2 within the paper.

DATA

To understand the interplay of volcanism and tectonic forces, volcanic space-time-composition patterns are key. Here we present new (Supplemental Table 1[1], yellow cells) and published data (Table 1; Supplemental Table 2[2]) that allow us to construct a longitudinal profile, and two latitudinal profiles across the Sierra Nevada mountain range. The new data include major oxide (n = 78), trace element (n = 26), and isotopic ($^{87}Sr/^{86}Sr$ and $^{143}Nd/^{144}Nd$; n = 109) compositions from the central Sierra Nevada and from Dixie Mountain (Figs. 1B and 2). Of special interest is whether and how Sierran space-time trends are affected as one moves north into the southern Cascades and east into the Walker Lane. Our analysis thus includes published data from volcanic fields in California (or Nevada, when such fields cross a state boundary) and so extend north to the Shasta–Medicine Lake area, and east into the Walker Lane belt (Table 1; Fig. 1B). The spatial profiles obtained from the new and published data point to profound geographical and temporal controls on Sierran volcanic compositions, and illustrate the modern extent of lithosphere degradation.

Data Filters

As noted by others (e.g., Leeman, 1970; Lum et al., 1989; Fitton et al., 1991; Farmer et al., 2002; Blondes et al., 2008), mafic Cordilleran volcanic compositions reflect mantle sources and processes, rather than crustal contamination. Except for the southern Sierra, the selection of rocks with MgO > 6% (or SiO_2 < 55%) provides an effective filter against crustal assimilation for most isotopes and trace elements. In the southern Sierra, we only use rocks with MgO > 10% (or SiO_2 < 50%), to guard against crustal contamination.

METHODS

Isotope ratios and trace element concentrations were determined at Carleton University and the Ontario Geological Survey inductively coupled plasma–mass spectrometry laboratory, Sudbury, respectively (see Cousens, 1996). New and published $^{143}Nd/^{144}Nd$ ratios are corrected for instrumental fractionation using $^{146}Nd/^{144}Nd$ = 0.72190. Major oxides were determined by X-ray fluorescence at the California State University at Fresno (see Busby et al., 2008b). Age dates, sample locations, and field relationships were described in Busby et al. (2008a, 2008b), Busby and Putirka (2009), Hagan et al. (2009), Koerner et al. (2009), and Roullet (2006).

To build on prior work on partial melting conditions (Van Kooten, 1980; Baker et al., 1994; Wang et al., 2002; Leeman et al., 2005; C.T. Lee, 2011, personal commun.), we use the Si activity barometers of Putirka (2008) and Lee et al. (2009). As a test of the barometers, we compare pressure-temperature (*P-T*) estimates for more than 440 experimental data saturated with olivine + orthopyroxene ± other phases (hydrous and anhydrous); here we calculated *T* rather than use experimental *T* as input, so as to mimic how the models are applied to natural samples (Figs. 3B, 3C). We observe little systematic error for *T* estimates, although Equation 4 in Putirka et al. (2007) is a more precise thermometer. However, the Lee et al. (2009) models overestimate *P* (*P* > 3 GPa); the Putirka (2008) barometer slightly underestimates *P* (>3.5 GPa), but is much more accurate, in the range of 3–5 GPa. Because volcanic rocks of the southern Sierra Nevada might not be saturated with orthopyroxene (opx) (Elkins-Tanton

[1]Supplemental Table 1. Excel File of geochemical data for volcanic rocks from the Central Sierra Nevada. If you are viewing the PDF of this paper or reading it offline, please visit http://dx.doi.org/10.1130/GES00728.S1 or the full-text article on www.gsapubs.org to view Supplemental Table 1.

[2]Supplemental Table 2. Excel File of geochemical data for volcanic rocks from the Sierra Nevada and California portion of the Walker Lane. If you are viewing the PDF of this paper or reading it offline, please visit http://dx.doi.org/10.1130/GES00728.S2 or the full-text article on www.gsapubs.org to view Supplemental Table 2.

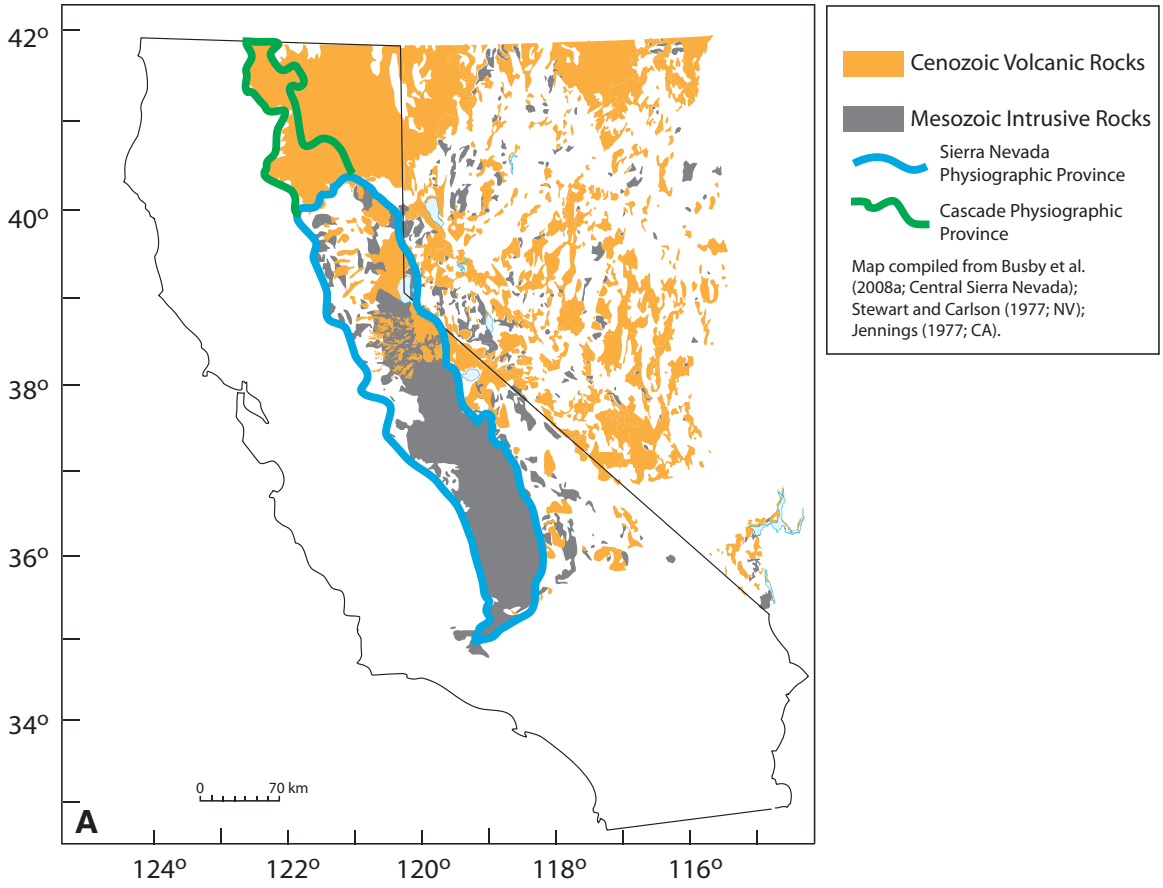

Figure 1 (*on this and following page*). (A) Map of Cenozoic volcanic and Mesozoic intrusive rocks in California and adjacent parts of Nevada. The Sierra Nevada physiographic province (blue line; Wakabayashi and Sawyer, 2001) transitions into the Cascades (green line) north of Lassen. Note that areal abundances of volcanic rocks increase dramatically moving to the north along the Sierra Nevada.

and Grove, 2003), we also test whether Si activity can be buffered by olivine (ol) + clinopyroxene (cpx) (Carmichael et al., 1970). We thus calculate *P* for 154 experimental liquids saturated with ol + cpx ± other phases, but without opx, using Equation 42 of Putirka (2008) and experimental *T* as input. For these experiments, errors are comparable to those for ol + opx–saturated experiments, indicating that the Putirka (2008) barometer can be applied to ol + cpx systems without recalibration (Fig. 3C).

We can only apply the Si activity barometers to rocks that have undergone no crustal assimilation, so we only consider rocks with MgO > 8% generally, and MgO > 10% for Pliocene southern Sierra volcanics (see Results and Discussion). Mafic whole-rock compositions are corrected by olivine addition (Fo_{90}) to achieve equilibrium with mantle olivine of $Fo_{90.54}$ (the highest Fo reported by Feldstein and Lange, 1999), at $K_D^{Fe\text{-}Mg} = 0.32$. These calculations assume mean $FeO/Fe_2O_3 = 0.74$ on a weight percent basis (from Feldstein and Lange, 1999), and our barometers use 2% H_2O in the primitive magma (Feldstein and Lange, 1999; Putirka and Busby, 2007; methods in Putirka et al., 2011). For comparisons of Fe, we use Fe_2O_3t (total Fe as Fe_2O_3), because most Sierran rocks are analyzed for Fe_2O_3t. At Lassen, FeOt is reported, and we recalculate Fe cations to obtain Fe_2O_3t, (for all practical purposes $Fe_2O_3t = FeOt/0.91$); this calculation has no implications for Fe^{3+}/Fe^{2+}, which undoubtedly varies widely in the Sierra (Feldstein and Lange, 1999).

We also estimate melting conditions based on trace element ratios. Garnet-bearing peridotite is only stable at >70–75 km, while spinel peridotite is stable at shallower depths (Longhi, 1995; Kinzler, 1997). Sm/Yb and Lu/Hf are effective for distinguishing between these sources because Yb and Lu are strongly compatible in garnet, but incompatible in spinel and other peridotite phases (e.g., Salters, and Longhi, 1999). For partial melting and fractional crystallization calculations, partition coefficients for major oxides are from Walter (1998) and Gaetani and Grove (1998). For trace elements, partition coefficients are from Salters and Longhi (1999) and Gaetani et al. (2003). Liquid compositions are calculated using fractional crystallization, partial melting (Rayleigh, 1896; Gast, 1968), and assimilation–fractional crystallization (AFC) models (DePaolo, 1981), and energy-constrained AFC (Bohrson and Spera, 2001). Amphibole fractionation models use mineral compositions from Blatter and Carmichael (2001) and trace element partition coefficients from Davidson and Wilson (2011) and Luhr and Carmichael (1980). Phlogopite-liquid partitioning is based on Righter and Carmichael (1996). Source compositions are taken from mantle xenoliths (Beard and Glazner, 1995; Lee et al., 2001; Lee, 2005). Mantle mineralogies are from Workman and Hart (2005) and Walter (1998) (spinel peridotite = 68% olivine, 10% clinopyroxene, 20% orthopyroxene, and 2% spinel; garnet peridotite = 61% olivine, 13% clinopyroxene, 21% orthopyroxene, and

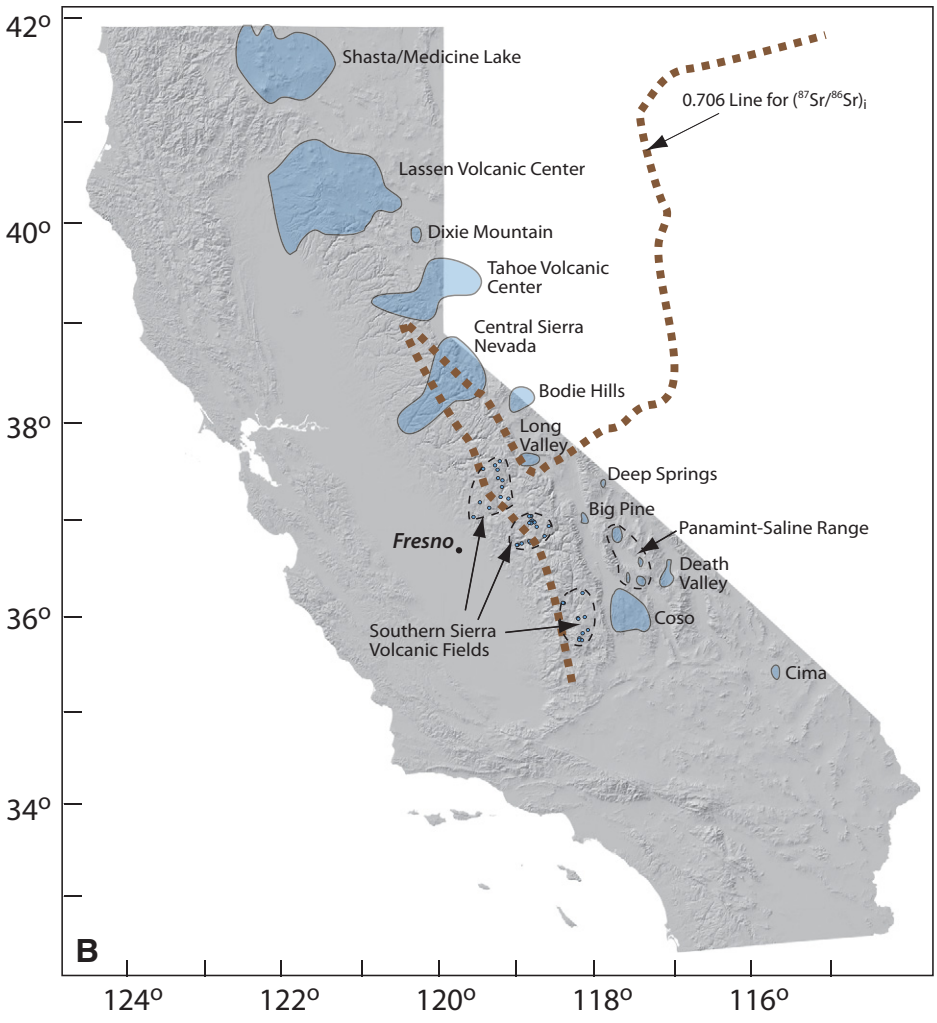

Figure 1 (*continued*). (B) Map of volcanic fields of Table 1, with placement of 0.706 line of Kistler (1990), adapted from Lackey et al. (2008).

5% garnet; for details see Putirka et al., 2011). Workman and Hart's (2005) model is used for an asthenosphere composition.

BACKGROUND AND PRIOR WORK

Volcanic centers of the Sierra Nevada have been the object of study for many decades, at least since Ransome's (1898) studies of the central Sierra Nevada. We provide a brief review of key aspects relevant to our study.

Tectonic Setting

The Mendocino and Rivera Triple Junctions formed when the Pacific-Farallon spreading ridge impinged North America ca. 30 Ma (Atwater, 1970; Glazner and Supplee, 1982). As the Mendocino Triple Junction (MTJ) migrates north, the Pacific–North American plate margin converts from a convergent to a transform boundary (the north-propagating San Andreas fault; Atwater, 1970), and arc-related volcanic activity ceases. This change yields the arc/post-arc transition documented in the ancestral Cascades (Cousens et al., 2008). To test for MTJ-related volcanic patterns, we calibrate the time at which the MTJ arrives at any given latitude:

$$\text{Age MTJ arrival (Ma)} = 184.5 - 4.57[\text{lat (°N)}] - 0.364[\text{lat (°N)} - 36.8443]^2. \quad (1)$$

Equation 1 is derived from the initial position of the MTJ at 30 Ma (29.65°N; Atwater, 1970) and MTJ positions of Atwater and Stock (1998; fig. 11 therein; note that the MTJ stalls in the Sierra at 4 Ma). To obtain paleo-MTJ latitude as a function of age, we have:

$$\text{MTJ latitude} = 40.4 - 0.213[\text{age (Ma)}] - 0.01[\text{age (Ma)} - 13.4]^2 - 0.0004[\text{age (Ma)} - 13.4]^3. \quad (2)$$

The regression error is ±1 Ma for Equation 1 and ± 0.2° for Equation 2. We use data from Snow and Wernicke (2000) to reconstruct latitudes of volcanic rocks in the southern Walker Lane, although in practice, most such rocks are so young that the corrections are trivial. Volcanic rocks erupted north of the MTJ are subduction related and noted as pre-MTJ in Table 1; those that erupt south of the MTJ (post-MTJ) do so after subduction has ended. Neogene volcanics of the Tahoe region and the central Sierra Nevada contain rocks that erupted both prior to and after MTJ arrival, and so are noted as transitional in Table 1.

Another tectonic aspect of interest is that the physiographic Sierra Nevada crosses a major tectonic boundary. In the central Sierra Nevada (Fig. 1) the locus of Mesozoic plutonism shifts to the east (Kistler, 1974) (Fig. 1), but the topographic crest of the range continues north as the range transitions into the Cascades (Wakabayashi and Sawyer, 2001). This structural boundary is evident in the initial $^{87}Sr/^{86}Sr$ $[(^{87}Sr/^{86}Sr)_i]$ and $^{143}Nd/^{144}Nd$ ratios of Mesozoic plutons (Kistler and Peterman, 1973; DePaolo and Farmer, 1984). For example, where $(^{87}Sr/^{86}Sr)_i > 0.706$, south and east of the central Sierra, older, thicker Precambrian continental crust (or sediments derived from such; Saleeby et al., 1987) and CML are presumed to underlie the range; where $(^{87}Sr/^{86}Sr)_i < 0.706$, younger accreted terranes underlie the Sierra. The importance of this boundary is evident in map views of bedrock geology (Fig. 1A). In the presence of a little-faulted Mesozoic batholith, Cenozoic volcanic rock outcrops are rare, but to the north volcanic rocks dominate the landscape. This outcrop pattern is not a product of erosion in the high parts of the range (Putirka and Busby, 2007; Busby and Putirka, 2009), but instead reflects the fact that local density contrasts have a profound impact on magma transport (Lister and Kerr, 1991). Even in Hawaii, where volcanic shields are dominantly basaltic, high-density picrites stagnate at the base of the crust (Garcia et al., 1995). In the southern Sierra Nevada, thick granitic crust clearly inhibits upward transport of all but the lowest density silicate liquids (Putirka and Busby, 2007).

Continental Versus Asthenosphere Mantle Sources, and Lithosphere Degradation

It is now well established that asthenosphere and CML can be distinguished based on isotope and trace element ratios. Leeman (1970, 1974)

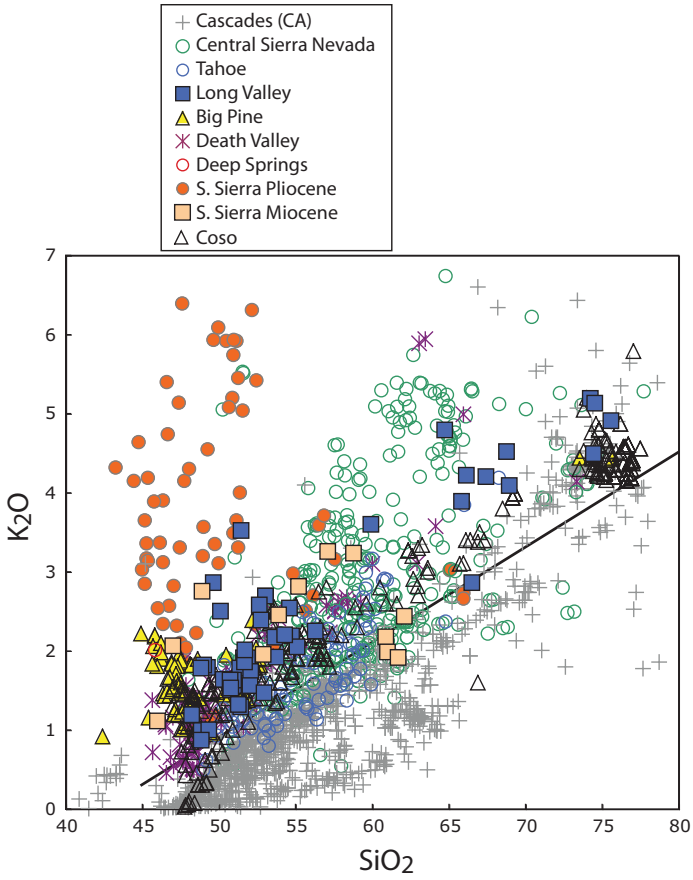

Figure 2. K_2O versus SiO_2. The rocks erupted in and adjacent to the Sierra Nevada span nearly the entire range of rock compositions erupted in much of the rest of the U.S. Cordillera. The empirical line [$K_2O = 0.12(SiO_2) - 5.1$] separates ~90% of Basin and Range rocks from ~90% of Cascade volcanics.

and Hedge and Noble (1971) were perhaps the first to recognize that elevated $^{87}Sr/^{86}Sr$ ratios (0.704–0.708, as in the Sierran Province of Leeman, 1974) in Cordilleran basalts require partial melting of CML that has been isolated from the convective mantle for 1–3 Ga. The idea of an enriched mantle source beneath the Sierra Nevada has since been verified by numerous subsequent studies of both volcanic rocks and xenoliths (e.g., Ormerod et al., 1991; Bradshaw et al., 1993; Beard and Glazner, 1995; Rogers et al., 1995; Cousens, 1996; Beard and Johnson, 1997; Blondes et al., 2008). Leeman (1970, 1974) further recognized that within the continental U.S., some basaltic rocks approach oceanic-like $^{87}Sr/^{86}Sr$ ratios (0.702–0.703); such rocks erupt after episodes of extensional strain, and so indicate replacement of older continental lithosphere with convective asthenosphere (e.g., Walker and Coleman, 1991; Fitton et al., 1991; Daley and DePaolo, 1992; DePaolo and Daley, 2000). Mantle sources can also be characterized by trace element ratios. CML is enriched in large ion lithophile elements (LILE) that are fluid mobile (e.g., Rb, Ba, Sr, Th, U, Pb), and depleted in high field strength elements (HFSE, e.g., Nb and Zr). These trace element signatures may have been imparted to the lithosphere by dehydration of the Laramide-age subducted slab (e.g., Rogers et al., 1995; Humphreys et al., 2003; Lee, 2005), or much earlier (Beard and Glazner, 1995), but in any case, CML has high LILE/HFSE ratios, such as high La/Nb, Th/Nb, and Ba/Zr, when compared to asthenosphere (e.g., Rogers et al., 1995; DePaolo and Daley, 2000; Plank, 2005).

Removal of CML is thought to be related to the development of the MTJ and the San Andreas fault system (Atwater, 1970; Atwater and Stock, 1998). In this model, upwelling asthenosphere may partially melt and erode CML. Ducea and Saleeby (1996, 1998a) first established key evidence in this regard, noting temporal and spatial changes in Sierran mantle xenoliths. In the southern Sierra, xenoliths hosted in 8–10 Ma volcanic rocks (to the west) contain garnet peridotite, while at the range front (to the east) volcanic rocks of 0.8–0.005 Ma host spinel peridotite. Lee et al. (2001) further showed that shallow-seated Miocene xenoliths are heated while deep-seated xenoliths are cooled. These observations indicate some form of mantle degradation in the Late Miocene, and removal of garnet-bearing lithosphere from beneath the range front by the Pleistocene.

Several observations, however, lead us to be skeptical of recent suggestions that lithosphere removal is complete beneath the Sierra Nevada (Frassetto et al., 2011), or that high K_2O Pliocene volcanics signal lithosphere removal (Farmer et al., 2002). Mantle xenoliths carried by Pleistocene volcanics at the range front have $^{87}Sr/^{86}Sr$ as high as 0.7065, and ε_{Nd} as low as –3.7, reflecting a mantle source that is ca. 820 Ma or older (Beard and Glazner, 1995). Van Kooten (1980) (see also Putirka and Busby, 2007) further suggested that southern Sierra Pliocene volcanics are derived by partial melting of garnet peridotite, which requires melting depths >70 km (Kinzler, 1997). Evidently, CML must have been retained beneath the range in the Pliocene. In the central Sierra, high K_2O volcanism is synchronous with range front faulting at 11–10 Ma (Putirka and Busby, 2007). High K_2O volcanism most likely signals episodes of high tensile stresses in the Walker Lane, which releases low F (where F is melt fraction) (high K_2O) magmas from the mantle (Putirka and Busby, 2007; Busby and Putirka, 2009; Takada, 1994).

RESULTS AND DISCUSSION

Given the current uncertainties of lithosphere degradation (as opposed to delamination, degradation encompasses both mechanical and chemical processes), we use volcanic space-time-composition patterns to reevaluate Sierran tectonics.

North-South Profile of Isotopic Compositions; Effects of Crustal Assimilation

New and existing isotope data for Sierran volcanics exhibit first-order spatial features that require explanation. Ratios of $^{87}Sr/^{86}Sr$ increase (Fig. 4A; unfiltered data) while $^{143}Nd/^{144}Nd$ ratios decrease (Fig. 4B) from Mount Shasta south to 37°N (e.g., Death Valley), and follow trends that match those for Mesozoic granitoids of the Sierra Nevada batholith. South of 37°N, this trend appears to reverse, but Death Valley and Coso volcanics, which have the lowest $^{87}Sr/^{86}Sr$

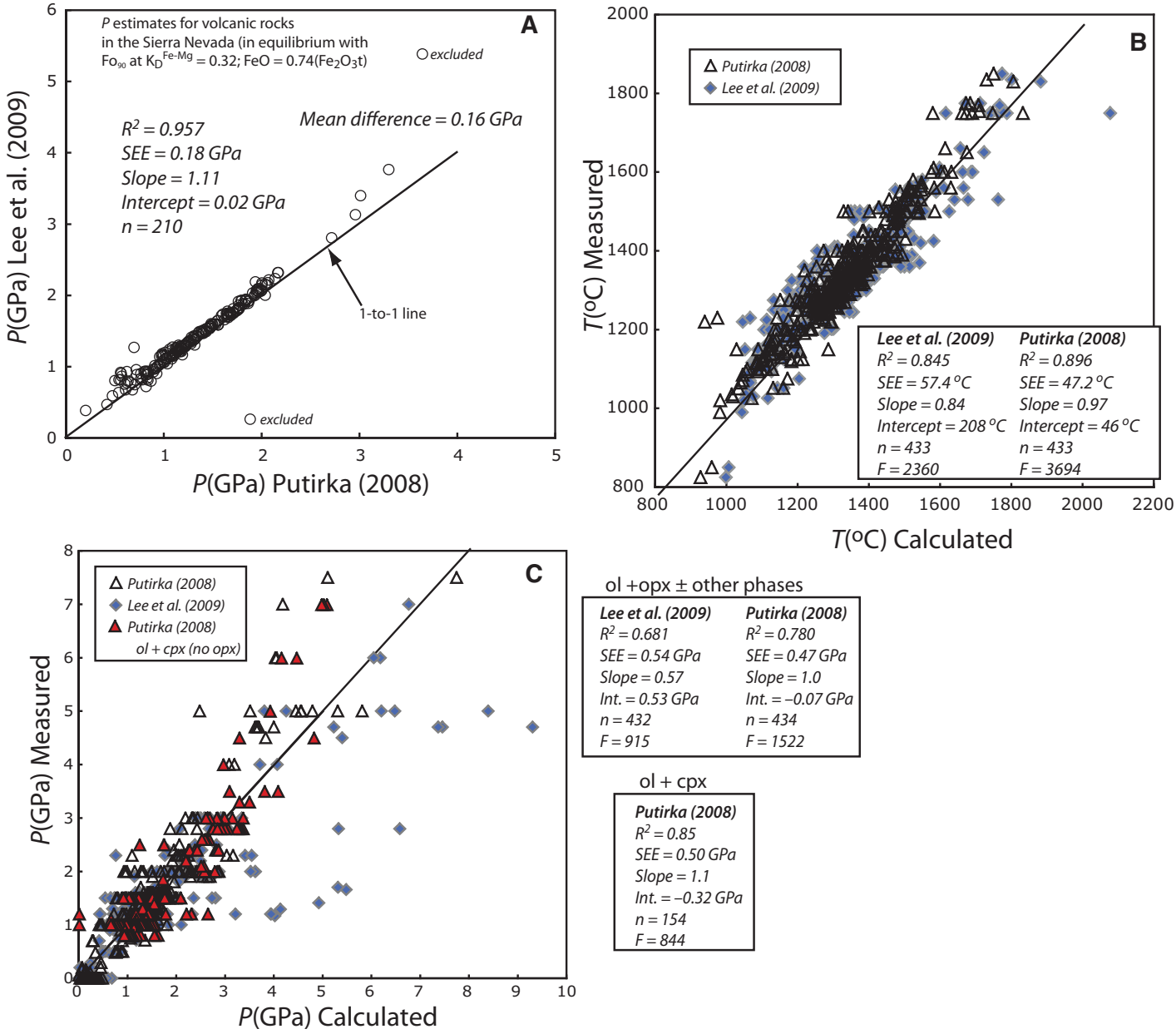

Figure 3. (A) Comparison of pressure (*P*) estimates using models of Lee et al. (2009) and Putirka (2008) for volcanic rocks from the Sierra Nevada. These methods yield nearly identical results at *P* < 2.5 GPa. (B) As a test for error, we compare temperature (*T*) estimates using these same models for experimental data; open triangles are *T* estimates using Putirka (2008; Eqn. 22 or Eqn. 4 from Putirka et al., 2007); blue diamonds are *T* estimates using Lee et al. (2009). (C) Comparison of *P* estimates for these same experimental data, using calculated rather than reported *T* as input, to mimic the calculation procedure for natural samples; open triangles are from Putirka (2008); blue diamonds are from Lee et al. (2009). In C, we also compare *P* estimates obtained (from Putirka, 2008) for liquids in equilibrium with olivine (ol) + clinopyroxene (cpx), but without orthopyroxene (opx) (red triangles). Experimental data are peridotite-saturated partial melting experiments, conducted between 1 atm and 11 GPa and 825 to 1850 °C, and are from the following: Agee and Draper (2004), Baker et al. (1994), Bartels et al. (1991), Blatter and Carmichael (2001), Bulatov et al. (2002), Draper and Green (1999), Draper and Johnston (1992), Dunn and Sen (1994), Elkins et al. (2000), Elkins-Tanton et al. (2003), Falloon and Danyushevsky (2000), Falloon et al. (2001, 1999, 1997), Feig et al. (2006), Fram and Longhi (1992), Gaetani and Grove (1998), Grove et al. (2003, 1982), Grove and Juster (1989), Hesse and Grove (2003), Holbig and Grove (2008), Juster et al. (1989), Kawamoto et al. (1996), Kelemen et al. (1990), Kinzler (1997), Kinzler and Grove (1992), LaPorte et al. (2004), Longhi (1995), Longhi and Pan (1988), Maaloe (2004), McDade et al. (2003), Meen (1990), Müntener et al. (2001), Mussel White et al. (2006), Parman et al. (1997), Parman and Grove (2004), Pichavant et al. (2002), Pickering-Witter and Johnston (2000), Ratajeski et al. (2005), Robinson et al. (1998), Salters and Longhi (1999), Schwab and Johnston (2001), Stolper (1980), Takagi et al. (2005), Takahashi (1980), Vander Auwera et al. (1994), Villiger et al. (2004), Wagner and Grove (1998), Walter (1998), Wasylenki et al. (2003), and Xirouchakis et al. (2001).

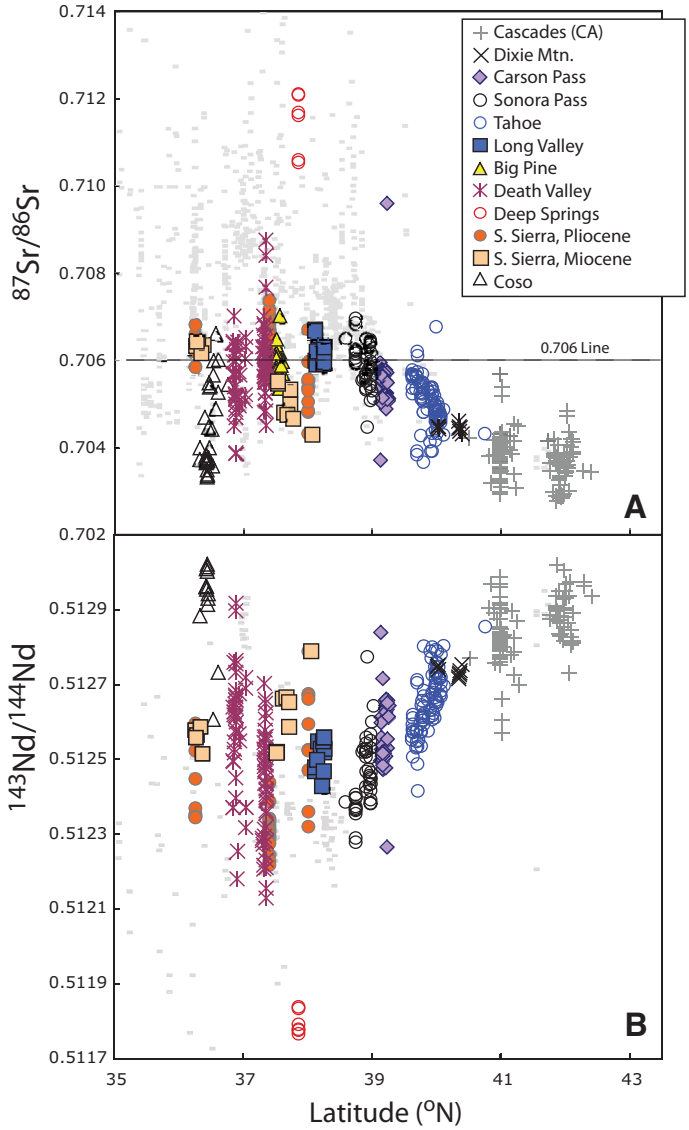

Figure 4. (A) Latitude versus $^{87}Sr/^{86}Sr$ for Sierran volcanic rocks. The 0.706 line is thought to mark the boundary between crust underlain by cratonic North American lithosphere (>0.706); this transition occurs for both Mesozoic intrusive and Cenozoic volcanic rocks, as noted by Kistler and Peterman (1973). (B) Latitude versus $^{143}Nd/^{144}Nd$ ratios for Sierran volcanic rocks; no filters applied to data; mafic basalts yield the same trends. These ratios follow the trend for Mesozoic granitoids, which are also shown.

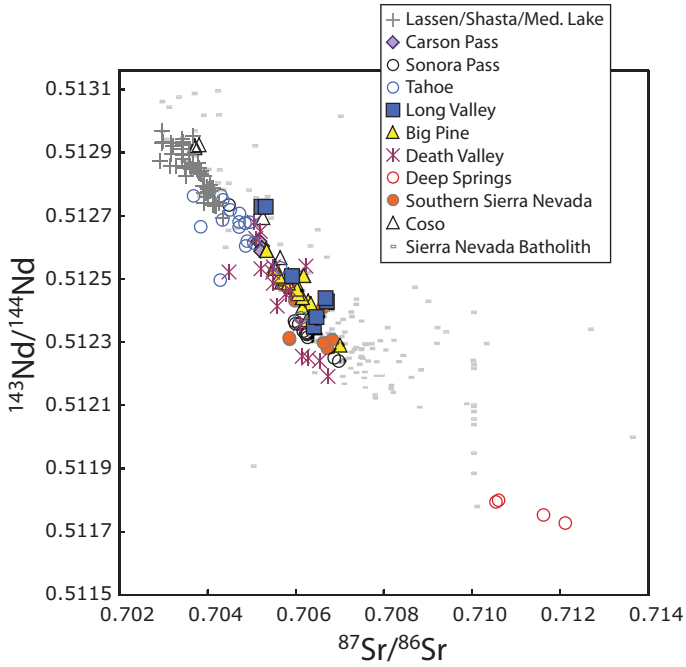

Figure 5. $^{143}Nd/^{144}Nd$ versus $^{87}Sr/^{86}Sr$ for Sierran volcanic rocks. Although some Sierran granitoids plot close to samples with the highest $^{87}Sr/^{86}Sr$ and lowest $^{143}Nd/^{144}Nd$, crustal assimilation cannot explain the linear trend since many rocks along this trend are very mafic, with MgO = 6–10 wt% and SiO_2 < 52 wt%.

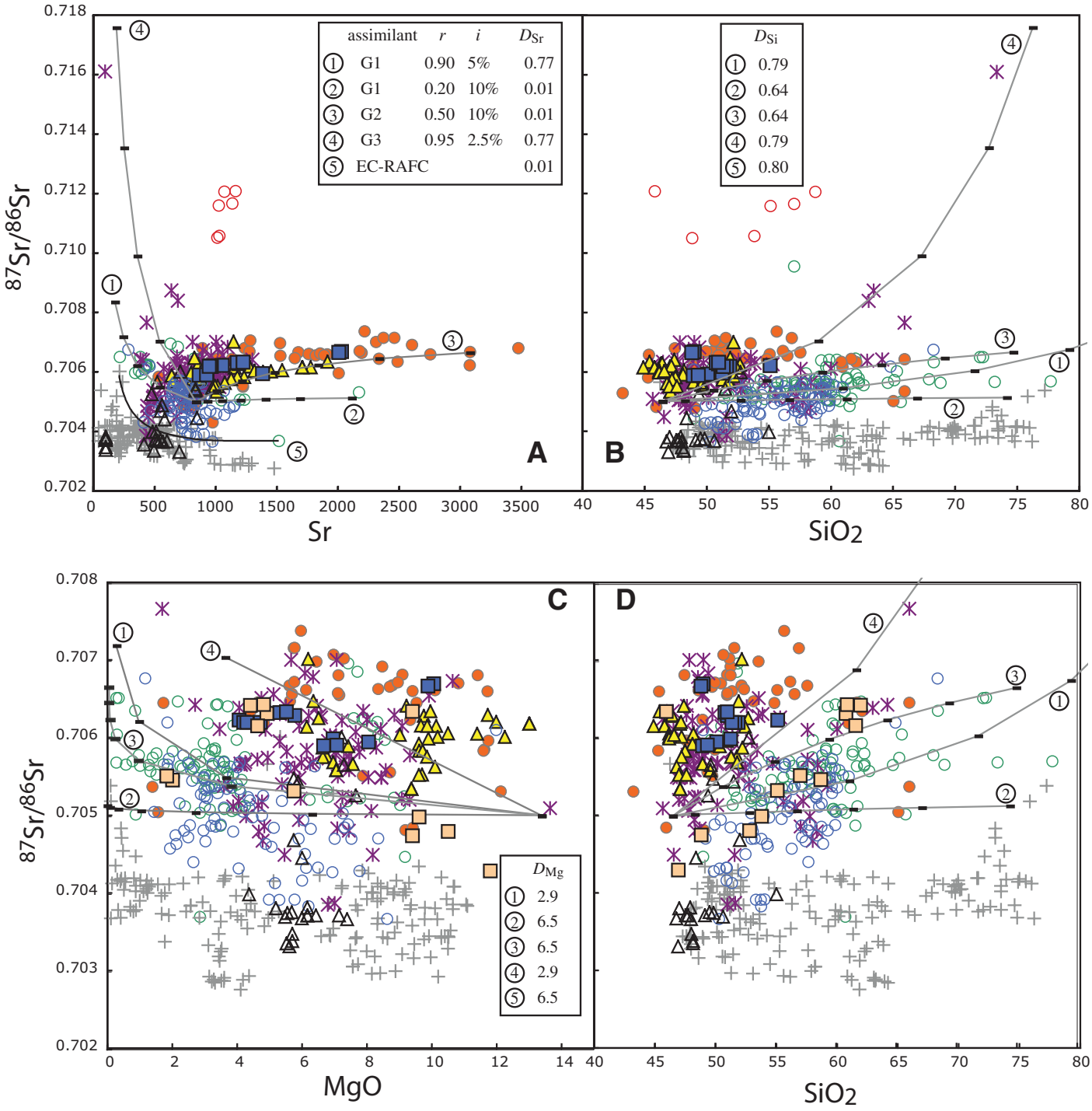

Figure 6 (*on this and following page*). Assimilation–fractional crystallization (AFC) models at a magnified scale. Symbols as in Figure 2. (A) $^{87}Sr/^{86}Sr$ versus Sr. (B) $^{87}Sr/^{86}Sr$ versus SiO_2. (C) $^{87}Sr/^{86}Sr$ versus MgO. (D) $^{87}Sr/^{86}Sr$ versus SiO_2. Each numbered curve represents an AFC model, where the initial composition is a mafic basalt approximating a mean composition of basalts from Feldstein and Lange (1999; this study); the EC-RAFC (energy-constrained recharge, assimilation, and fractional crystallization) model uses sample JHCP-20 as a starting liquid composition (which has the lowest $^{87}Sr/^{86}Sr$ in the central and southern Sierra Nevada; from Putirka et al., 2011). For wall-rock assimilants, G1 is a granitoid from Kylander-Clark et al. (2005; sample 074713), which has 73% SiO_2, 106 ppm Sr, and $^{87}Sr/^{86}Sr = 0.712$; G2 is sample DVB-108 from Ramo et al. (2002), which has 67.9% SiO_2, 687 ppm Sr, and $^{87}Sr/^{86}Sr = 0.71$. The value *r* = mass rate of assimilation/mass rate of crystallization; D_j are bulk distribution coefficients for element (or oxide) j, assuming olivine-only crystallization for curves 2, 3, and 5, and olivine (0.13) + plagioclase (0.4) + clinopyroxene (0.2) + hornblende (0.2) + apatite (0.02) + magnetite (0.05) for curves 1 and 4; the mineral assemblage for curves 1 and 4 are derived so as to simultaneously describe major element trends (Fig. 7). The value *i* gives the increments at which melt fractions (*F*) are calculated for each curve, with *F* = 1.0 (equal to the parental magma) where the curves converge.

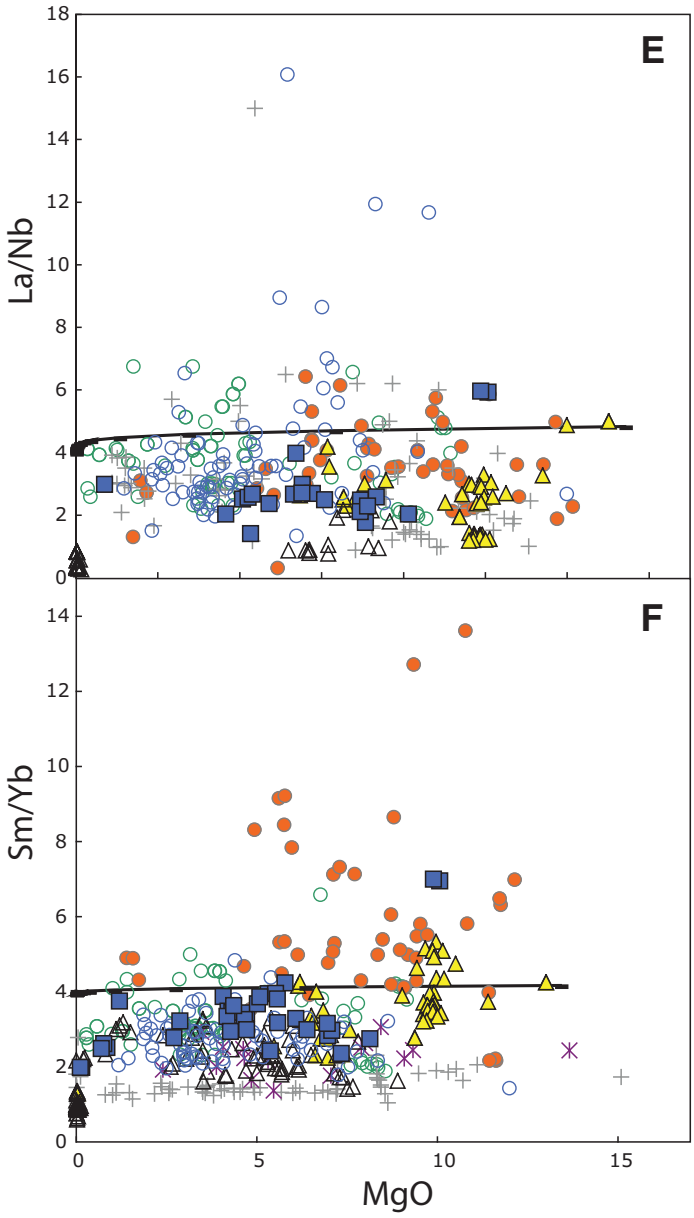

Figure 6 (*continued*). (E) La/Nb versus MgO. (F) Sm/Yb versus MgO. E and F show that key trace element ratios, indicative of source enrichments (La/Nb) and source mineralogy (Sm/Yb), are invariant with respect to MgO, and so are largely unaffected by AFC processes (AFC curve 2 is shown in both panels). AFC curves emanating from an arbitrary Sierran parental magma illustrate the AFC slopes that are possible over a range of values for *r* and D_j (Fig. 6A–D). A few samples (from the central Sierra Nevada and Death Valley) have <500 ppm Sr and trend toward $^{87}Sr/^{86}Sr$ of 0.707–0.716 (curves 1 and 4, Fig. 6A), and can be explained by large amounts of crustal assimilation ($r > 0.9$, $F < 0.5$; using sample TD17 from Feldstein and Lange, 1999, as a parent magma). Felsic rocks can be produced if D_{Sr} approaches 1 (i.e., if plagioclase is part of the fractionating assemblage) and *r* is low (<0.3), which yields the observed large increases in SiO_2 and limited increases in Sr and $^{87}Sr/^{86}Sr$.

and highest $^{143}Nd/^{144}Nd$, are younger than 6 Ma and erupted in the Walker Lane, a region of high extensional strain (e.g., DePaolo and Daley, 2000). Unusual volcanic rocks at Deep Springs (Beard and Glazner, 1998) also define isotopic extremes. However, within the Sierra Nevada there is no reversal, but a flattening of isotopic trends from 37°N to 35.75°N. All volcanic isotopic ratios plot on a single near-linear trend (Fig. 5), indicative of two-component mixing between an asthenosphere-like source exemplified by mafic Cascades lavas, and an enriched source. Sierra granitoids, however, cannot represent the enriched component (Figs. 5 and 6): many volcanic rocks with high $^{87}Sr/^{86}Sr$ and low $^{143}Nd/^{144}Nd$ have high MgO (>8 wt%) and low SiO_2 (<50%; see following discussion), and Pliocene southern Sierra volcanics with high Sr and moderate $^{87}Sr/^{86}Sr$ contents cannot be generated by AFC because AFC predicts higher than observed SiO_2 and lower than observed MgO (Fig. 6). AFC of felsic crust explains evolved compositions, with $SiO_2 > 57\%$ for Pliocene lavas, and $SiO_2 > 62\%$ and $MgO < 6\%$ for most other flows (see following discussion). Mafic volcanic rocks, however, must inherit their isotopic character from the mantle (Leeman, 1970; Ormerod et al., 1988; Lum et al., 1989; DePaolo and Daley, 2000; Blondes et al., 2008), as do their Mesozoic plutonic counterparts (Kistler, 1990).

Partial Melting, Assimilation, and Magma Evolution from Major and Trace Elements

Sierran volcanics exhibit key contrasts in major oxides, which can be used to decipher the conditions of mantle melting. Most volcanics have very similar MgO-SiO_2, MgO-Fe_2O_3t, MgO-Al_2O_3, and MgO-CaO trends (Fig. 7). However, southern Sierra volcanics have distinctly low Al_2O_3 and CaO at high MgO compared to other Sierran lavas. Southern Sierra volcanics are also the most enriched in TiO_2, Na_2O, K_2O, and P_2O_5 at high MgO. Also distinct are Walker Lane volcanics at Coso, Death Valley, Long Valley, and Big Pine, which are enriched in TiO_2, K_2O, and/or P_2O_5. As with $^{87}Sr/^{86}Sr$, AFC processes are incapable of generating elevated TiO_2, Na_2O, K_2O, or P_2O_5 at high MgO (Fig. 7); either source-region enrichments or low degrees of partial melting (low *F*) are required. As to the latter, partial melts of Sierran peridotite xenoliths (Mukhopadhyay and Manton, 1994; Beard and Glazner, 1995) explain elevated TiO_2, Na_2O, K_2O, and P_2O_5 when $F = 0.08–0.01$ (Fig. 7). In addition, low Al_2O_3 and CaO contents for southern Sierra magmas are simultaneously explained, if 2%–5% garnet is retained in the mantle residue. These results are in agreement with prior work (Van Kooten, 1980; Dodge and Moore, 1981; Lange and Carmichael, 1996) and consistent with the idea that tensile stresses (in the Walker Lane) favor eruption of low-*F* magmas (Takada, 1994; Putirka and Busby, 2007).

Rocks with >10% MgO are primitive enough to plot on an olivine control line (FC1 in Fig. 7) (see Powers, 1955; Wright and Fiske, 1971). This is evidenced by near-constant Fe_2O_3t at

high MgO, which indicates that the bulk distribution coefficient for Fe, $D_{Fe} \approx 1$ (so olivine is the only phase to precipitate). More evolved compositions are best explained as mixtures of liquids produced along curve FC1, followed by subsequent AFC involving precipitation of olivine + clinopyroxene + plagioclase + hornblende + magnetite + apatite (AFC curve in Fig. 7). Hornblende is likely a ubiquitous fractionating phase at $SiO_2 > 54\%$, at least in the central Sierra Nevada. Davidson et al. (2007) showed that Dy/Yb versus SiO_2 (Fig. 7I) is an effective means to identify hornblende (hbl) fractionation, since $D_{Dy}^{hbl\text{-}liquid} > D_{Yb}^{hbl\text{-}liquid}$, leading to decreases in Dy/Yb with increased SiO_2. Southern Sierra and Long Valley lavas do not exhibit internal SiO_2-Dy/Yb variations, but most Sierran lavas south of Lassen plot on a hornblende fractionation trend (Fig. 7I) emanating from those compositions. Volcanic rocks from the Cascades (Lassen, Shasta, Medicine Lake) have much lower Dy/Yb at low SiO_2. Given that CML is likely absent beneath Lassen, the lithosphere is probably less thick there, and so lower Dy/Yb reflects spinel peridotite partial melting (curve PM3), whereas thicker, colder CML to the south allows for a greater contribution from garnet peridotite–derived partial melts (curve PM1, Fig. 7I) yielding higher Dy/Yb ratios.

Figure 7 (*on following three pages*). Variation diagrams (anhydrous totals for experiments and natural data) of MgO versus (A) SiO_2, (B) Fe_2O_3t (= Fe_2O_3 total, calculated as FeOt/0.9 for Lassen), (C) Al_2O_3, (D) CaO, (E) TiO_2, (F) Na_2O, (G) K_2O and (H) P_2O_5 and SiO_2 versus Dy/Yb (I). Several curves illustrate fractional crystallization (FC), assimilation–fractional crystallization (AFC), partial melting (PM) and mixing (M) models. PM1 and PM2 are partial melting curves; melt fractions are indicated in each panel. Both use xenolith compositions from Beard and Glazner (1995; sample Pi-2–67) and Lee (2005) as starting compositions (K_2O = 0.06 wt%; Na_2O = 0.28%; TiO_2 = 0.17%; P_2O_5 = 0.03%). In (G) and (H), longer hachure marks show melt fractions for the case that starting compositions have K_2O = 0.09% and P_2O_5 = 0.05%. PM1 uses a residual mineralogy of 53.1% olivine + 1.9% garnet + 27.3% clinopyroxene, + 17.7% orthopyroxene, taken from experiment 30.05 from Walter (1998; P = 3.0 GPa; T = 1500 °C; F (melt fraction) <5%). In (C), PM2 has garnet increased to 5% at the expense of olivine, which better explains low Al_2O_3 in the southern Sierra suite. FC1 assumes olivine-only fractionation and a mean mafic composition from the central and southern Sierra Nevada. FC2 uses a 30% olivine + 70% clinopyroxene fractionation assemblage, and uses a 2% melt from either PM1 or PM2 as a starting composition. FC3 begins with a 5% partial melt from PM1, also followed by fractional crystallization of 30% olivine + 70% clinopyroxene (optimized to reproduce high TiO_2 compositions at Coso). M is a mixing curve between our mean Sierran mafic parental magma and the melt produced at F = 0.6 along curve FC1. The AFC curve uses a 50–50 mixture along curve M as a starting liquid; the AFC curve here is the same as in AFC curve 1 in Figure 6, but with r = 0.8 (mass rate of assimilation/mass rate of crystallization), optimized to produce highly evolved Sierran lava compositions by migrating through the Sierran major element trends. In (I), Dy/Yb versus SiO_2 is used to test for amphibole fractionation (Davidson et al., 2007). For basaltic samples (SiO_2 < 53%) Cascade lavas have lower Dy/Yb, consistent with partial melting of spinel peridotite (PM3; 58% olivine, 14% clinopyroxene, 23% orthopyroxene, 2% spinel; Workman and Hart, 2005) rather than garnet peridotite (PM1); the steep drop in Dy/Yb with increased SiO_2 exhibited by Tahoe and central Sierran lavas is best explained using $D_{Dy}^{hbl\text{-}liq}$ = 2.6 (Luhr and Carmichael, 1980). As noted, high TiO_2 contents at Coso and Big Pine require low F (2%–5%) parental magmas, but at Coso, high TiO_2 can be explained by subsequent fractionation of a clinopyroxene-rich assemblage (30% olivine + 70% clinopyroxene), which is an abundant phenocryst phase (Mordick and Glazner, 2006). Clinopyroxene fractionation is not steep enough, however, to connect minimum and maximum TiO_2 contents, even when Ti is assumed to be highly incompatible (D_{Ti} < 0.1), and so intrasuite variations in source compositions or F are still required.

Mantle Source Mineralogy and Composition

The latitudinal patterns of Figure 4 clearly indicate at least two mantle sources: one with time-integrated enrichments of Sm/Nd and Rb/Sr to the south and another lacking such enrichments to the north. Are such contrasts accompanied by contrasts in mantle mineralogy (pyroxenite or phlogopite-bearing peridotite) or degree of fluid-based enrichments, such as K-metasomatism (see models by Van Kooten, 1980; Feldstein and Lange, 1999; Farmer et al., 2002)?

As to metasomatism, no special enrichments are evident. Indices of fluid enrichments in the Cordillera (e.g., Rogers et al., 1995; DePaolo and Daley, 2000), like La/Nb and Th/Nb ratios, decrease from north to south (Figs. 8A, 8B), while Ba/Zr ratios are approximately constant (Fig. 8C), even though Ba is highly enriched in many southern Sierran volcanics (Fig. 9A). These relationships do not support the idea that high K_2O volcanics in the central and southern Sierra derive from an especially fluid-metasomatized source. Either enrichments along the Sierra are equal (Ba), or some fluid-mobile elements (Th, La) were actually lost from the southern Sierran mantle prior to late Cenozoic volcanism.

As to a phlogopite-bearing mantle, Dodge and Moore (1981) rejected such a source because K/Rb ratios are too high in southern Sierra volcanics. As a further test, we compare K and Ba, which are both highly compatible in phlogopite (Righter and Carmichael, 1996), to Sr and Rb, respectively. A phlogopite-bearing residue should yield basalts with low Ba/Rb and high Sr/K_2O, but partial melts of a source with just 0.5% residual phlogopite yield liquids with Ba/Rb ratios that are too low to explain Sierran volcanic rocks with MgO > 6% (Fig. 9A), even when using a source that has the highest Ba contents observed among all Cordilleran mantle xenoliths (Lee, 2005). This might appear to contradict results from Elkins-Tanton and Grove (2003), but those experiments do not yield a multiple saturation point that contains garnet, which we know must be a residual phase for Sierran Pliocene volcanics (Dodge and Moore, 1981; Van Kooten, 1980; Putirka and Busby, 2007; this study). Therefore, the Elkins-Tanton and Grove (2003) multiple saturation point cannot represent a residual mantle source for these rocks; their work, however, sheds light on the conditions at which phlogopite is stable in the mantle. At depths of 100 km, phlogopite only occurs if $H_2O \geq 6$ wt%, much greater than the 2% H_2O needed for eruption (Feldstein and Lange, 1999; Putirka and Busby, 2007) or the 3–5 wt% H_2O estimated by Feldstein and Lange (1999), based on phlogopite barometry and saturation (Righter and Carmichael, 1996). A key misunderstanding appears to be that because phlogopite occurs in a volcanic rock, it must therefore be present in the mantle source. Leucite provides a perfect counterexample: it is present in high K_2O volcanics both as a groundmass (e.g., Van Kooten, 1980; Feldstein and Lange, 1999) and phenocryst phase (Beard and Glazner, 1998), and yet no proposal for a leucite-saturated mantle has

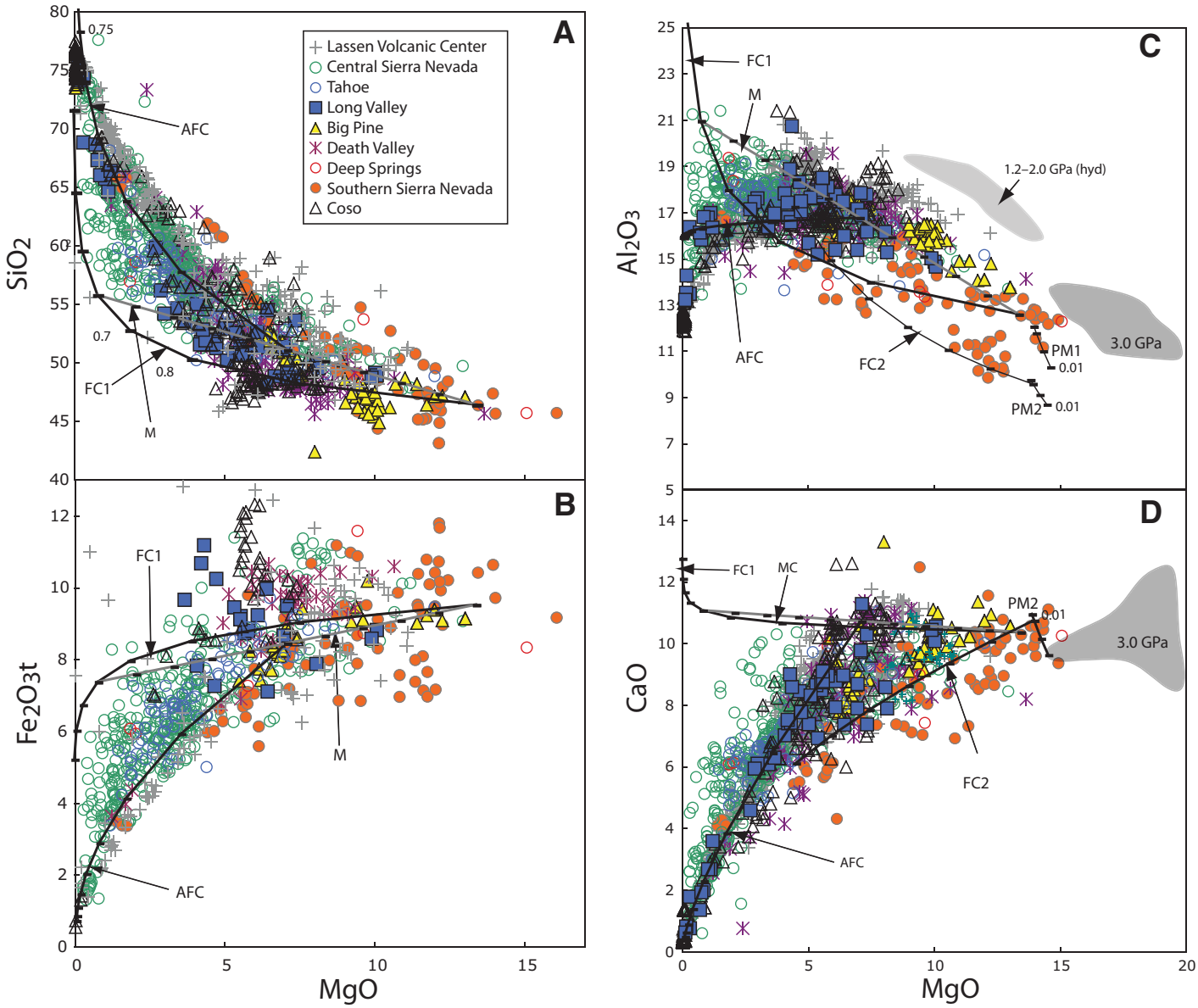

Figure 7.

been made. Rather, both leucite and phlogopite form as precipitates from high K_2O liquids after their removal from their mantle sources, a result supported by the absence of phlogopite in mantle peridotites (e.g., Beard and Glazner, 1995) that contain as much as 0.09% K_2O, i.e., more than enough K_2O to explain the highest K_2O in Sierran volcanics ($F \approx 2\%$).

A pyroxenite source can also be rejected for most Sierran volcanics. If pyroxenite sources represent ancient partial melts trapped in the mantle (e.g., Leeman and Harry, 1993), they should have high Rb/Sr and $^{87}Sr/^{86}Sr$ and yield partial melts with high Sm/Yb. However, in the central Sierra Nevada $^{87}Sr/^{86}Sr$ does not vary with Sm/Yb. In addition, using $D_{Sr}^{cpx\text{-}liq} = 0.1$ (e.g., Gaetani et al., 2003), even the most Sr-rich pyroxenite xenolith from Lee et al. (2006) yields Sr and Sr/K_2O ratios that are too low compared to natural lavas (Fig. 9B). Experiments on high K_2O liquids (Schmidt et al., 1999) yield $D_{Sr}^{cpx\text{-}liq} > 0.3$, making the problem worse. However, while such a source is unnecessary, we cannot exclude a garnet pyroxenite source for high Sm/Yb and high K_2O Pliocene volcanics.

In any case, partial melts of Sierran peridotite xenoliths (Mukhopadhyay and Manton, 1994; Beard and Glazner, 1995; Lee, 2005) explain all major and trace elements in Sierran volcanics. Big Pine and Oak Creek peridotite xenoliths, for example, explain high K_2O, TiO_2, Na_2O, and P_2O_5 if $F \approx 1\%–3\%$ (Figs. 7E–7H). Whereas the mean of Sierran peridotite xenoliths (Lee, 2005) has insufficient Ba (curve C, Fig. 9A), xenolith Ki5–8B (Cima) has more than enough Ba (curve A) to explain volcanic compositions. Similarly, while Ki5–8B has insufficient Sr, the mean of peridotite xenolith compositions explains Sr remarkably well (Fig. 9B). These results show clearly that (1) the Sierran mantle is enriched (Lee, 2005), (2) variations in F, rather than special local source enrichments (Moore and Dodge, 1980; Van Kooten, 1980), control volcanic compositions, and (3) heterogeneities in the Sierran basalt source region are

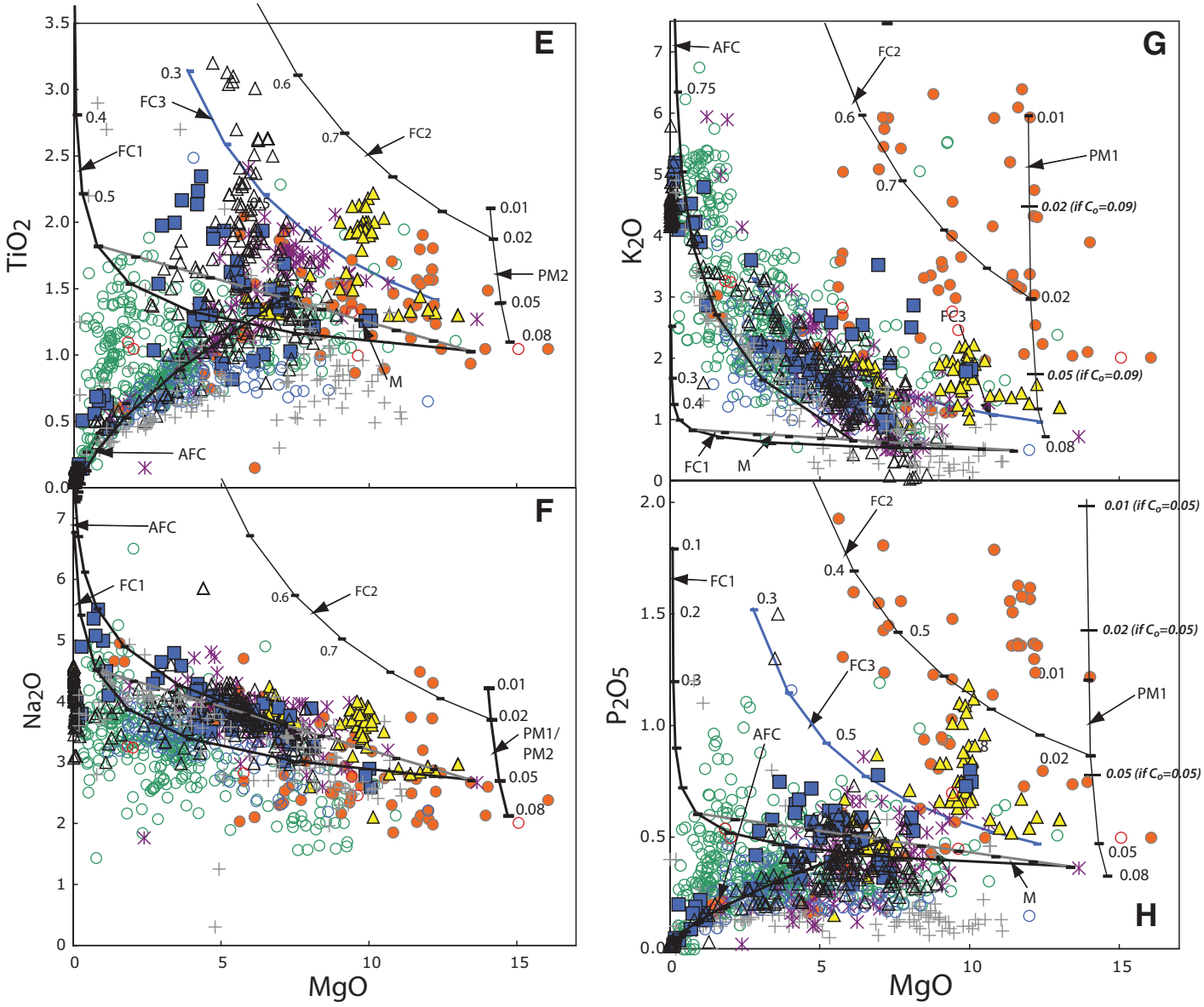

Figure 7 (*continued*).

encompassed by peridotite xenoliths from the region, so do not require special residual mantle mineralogies.

Depths of Melt Extraction from the Mantle

Because enriched CML exists in most Sierran volcanic source regions, at least south of 39.6°N (Tahoe area) (Fig. 4), thermobarometry can be used to delimit the depths at which CML is located. Van Kooten (1980) used an early version of the Si activity barometer (Nicholls et al., 1971), and derived melt extraction estimates of 3.3 and 4.1 GPa (100–125 km) for two southern Sierra volcanic samples. Those estimates imply that removal of garnet-bearing lithologies beneath the Sierra could not have been complete until after the Pliocene. Farmer et al. (2002) suggested that melt extraction occurs at ~40 km, based on phlogopite phenocryst barometry of Feldstein and Lange (1999), who computed pressures of 1.2–1.6 GPa, equal to depths of 44–57 km [for the Sierra Nevada we use: depth (km) = 9.69 + 3.03 P + 0.00054$(P - 32.736)^2$ + 0.0001714$(P - 32.736)^3$ – 0.0000037$(P - 32.736)^4$, where P is in kbar]. However, as shown, the mantle source did not contain residual phlogopite (Fig. 9). The 40 km depth estimate from phlogopite phenocrysts instead indicates ponding of magma at the base of the Sierran crust (40 km; Fliedner and Ruppert, 1996). To test this idea, we calculate *P-T* conditions for clinopyroxene phenocrysts from Feldstein and Lange (1999; using methods in Putirka et al., 2003): one clinopyroxene formed at nearly atmospheric pressure (0.1 kbar), while three others yield a mean of 14.8 ± 0.03 kbar, and another three yield an average of 10.6 ± 0.16 kbar. These latter pressures correspond to depths of 53 and 39 km, respectively, and are equivalent to crust thickness within model error (±10 km), although the 53 km estimate may indicate partial crystallization in the uppermost mantle, which is not uncommon (Putirka, 2008; Putirka and Condit, 2003; Mordick and Glazner,

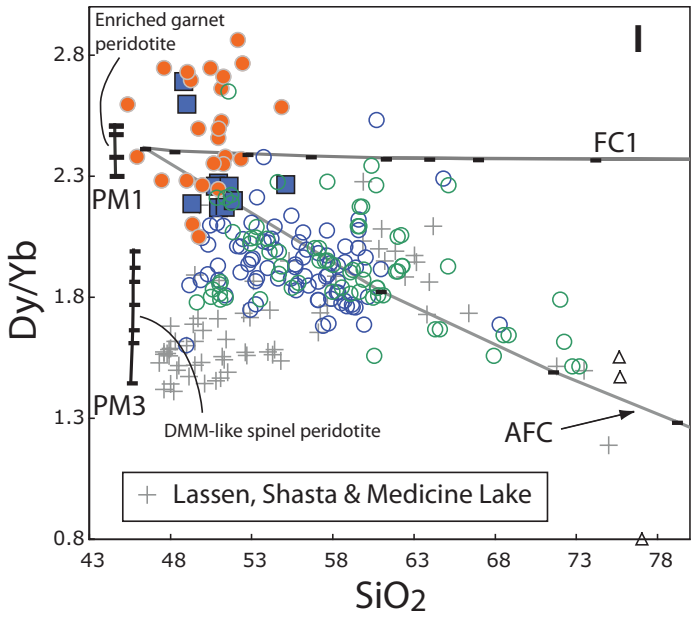

Figure 7 (*continued*).

2006). To better examine mantle melt extraction depths, we use Sm/Yb and Lu/Hf ratios and Si activity models.

Pliocene rocks from the southern Sierra have the highest Sm/Yb and lowest Lu/Hf ratios observed among all mafic volcanics in the Sierra Nevada (Figs. 10A, 10B). Both ratios require partial melting of a garnet-bearing source, which also explains low Al_2O_3 at high MgO (Fig. 7C), and elevated Dy/Yb at low SiO_2 (Fig. 7I). Most other Sierran volcanics have Sm/Yb and Lu/Hf ratios that indicate partial melting in the spinel peridotite field, or mixtures of spinel peridotite and garnet peridotite partial melts. We emphasize that these latter models are not unique: at Big Pine, a contribution from a garnet peridotite source appears required when using a mean Sierran xenolith mantle composition (e.g., Sm = 0.6 ppm, Yb = 0.12 ppm). However, if we reduce Yb in the source to 0.2 ppm Yb, which is well within the observed range for Sierran xenoliths (Lee, 2005), Sm/Yb ratios from spinel peridotite partial melts are >5 and have >2.3% K_2O, and so explain both Sm/Yb ratios and Yb and K_2O concentrations. Southern Sierra volcanics, however, are a different matter. Even the most infertile xenolith compositions (from Lee, 2005), with the lowest Yb and Lu contents, fail to yield the lowest Lu/Hf and highest Sm/Yb ratios in the southern Sierra. Moreover, such infertile sources would yield magmas with much lower than observed CaO (Fig. 10C), and vastly lower Yb (<0.24 ppm, compared to the observed 0.4–2.2 ppm) and Lu (<0.03 ppm, compared to observed 0.1–0.3 ppm). In any case, the Sierran mantle is probably not so depleted. South of Lassen, Al_2O_3 contents vary widely but CaO contents are similar (Fig. 10D), indicating that highly infertile sources are absent. We thus conclude that southern Sierra volcanics require a garnet peridotite source, while other Sierran lavas are derived from a spinel peridotite source (<75 km), ± mixing of garnet peridotite–derived melts (>75 km).

Si activity barometers (Putirka, 2008; Lee et al., 2009) provide an independent test of trace element–based results. These barometers yield remarkably similar *P-T* estimates for most Sierran volcanics (Fig. 11A). Pressure estimates are closest [*P* of Lee et al. (2009) – *P* of Putirka (2008) = 0.11 GPa on average) when the Putirka (2008) barometer is matched with the thermometer of Equation 4 from Putirka et al. (2007). However, the differences are increased only slightly when using the thermometer of Equation 2 from Putirka et al. (2007) [*P* of Lee et al. (2009) – *P* of Putirka (2008) = 0.15 GPa on average], and are closer still at <3 GPa. These tests indicate that our *P-T* estimates are robust at $P \leq 3$ GPa, and our estimates of 44–74 km at Big Pine are remarkably close to the 40–75 km estimates of C.T. Lee (2011, personal commun.).

Melt extraction depths fall into two groups. Samples from Lassen yield a mean of 33 ± 9.7 km [for Lassen, depth (km) = $0.0007P^3 - 0.0408P^2 + 3.8266P + 0.3476$, where *P* is in kbar], while remaining Sierran suites yield 40–75 km depths (53 ± 15 km on average). *P* estimates positively correlate with Sm/Yb (Fig. 11A), which indicates that Sm/Yb is a valid proxy for mean depth of melt extraction. Some samples from the southern Sierra, however, exhibit a low *P* compared to their high Sm/Yb (Fig. 11A), but since even high MgO southern Sierra volcanics are affected by crustal assimilation (Fig. 5; Farmer et al., 2002; Ducea and Saleeby, 1998b), calculated *P* may be too low. For example, K_2O/P_2O_5 is a recognized index of crustal assimilation (e.g., Farmer et al., 2002) and southern Sierra samples plot between a southern Sierran basalt and granitoid (Fig. 11B) along a mixing curve for K_2O/P_2O_5 versus *P*. The effect of AFC is to increase SiO_2, which lowers calculated *P* by as much as 2–3 GPa in this case (note that MgO is nearly 8%, even at *F* = 60%). In contrast, assimilation has almost no effect on Sm/Yb (Fig. 11A).

These results, in combination with isotope ratios, require partial melting of CML (Figs. 8 and 9) 40–75 km beneath the modern range front and central Sierra, and 40–110 km beneath the southern Sierra during the Pliocene (Fig. 12). These estimates allow for loss of garnet-bearing mantle from beneath the range front, but indicate that garnet-bearing CML was present during the eruption of Pliocene Sierran magmas.

Implications for Lithosphere Removal

Taken together, these results indicate that the transition from a mantle wedge beneath Lassen to thick, cold CML beneath the southern Sierra provides a primary control on volcanic rock compositions. First, depths of melt extraction from the mantle (Fig. 13B) are greater to the south than to the north. Second, just as isotope ratios shift to CML-like values to the south (Fig. 4), in rocks with >8% MgO, concentrations of incompatible elements and oxides, like K_2O (Fig. 13A), increase to the south (Putirka and Busby, 2007), indicating lower degrees of partial melting in that direction. Third, indices of fluid inputs (e.g., La/Nb) do not vary with depth of melt extraction (Fig. 13C). Fourth, isotope ratios fall into two groups: a mostly northern low-*P* suite, which approaches mid-oceanic ridge basalt mantle–like isotope ratios, and a southern high-*P* suite, with a CML signature (Figs. 13D, 13E). Mesozoic granitoids show a similar isotope-space pattern (Figs. 3 and 13B; Kistler and Peterman, 1973; DePaolo and Farmer, 1984). In concert, these observations indicate greater partial melting depths and lower *F* beneath thicker, and presumably cooler, lithosphere to the south, with little depth or spatial control on mantle enrichments. Since melting depths are everywhere as shallow as 40 km, CML heating reaches the base of the crust, which may result from a pervasive intrusion of asthenosphere or asthenosphere-derived partial

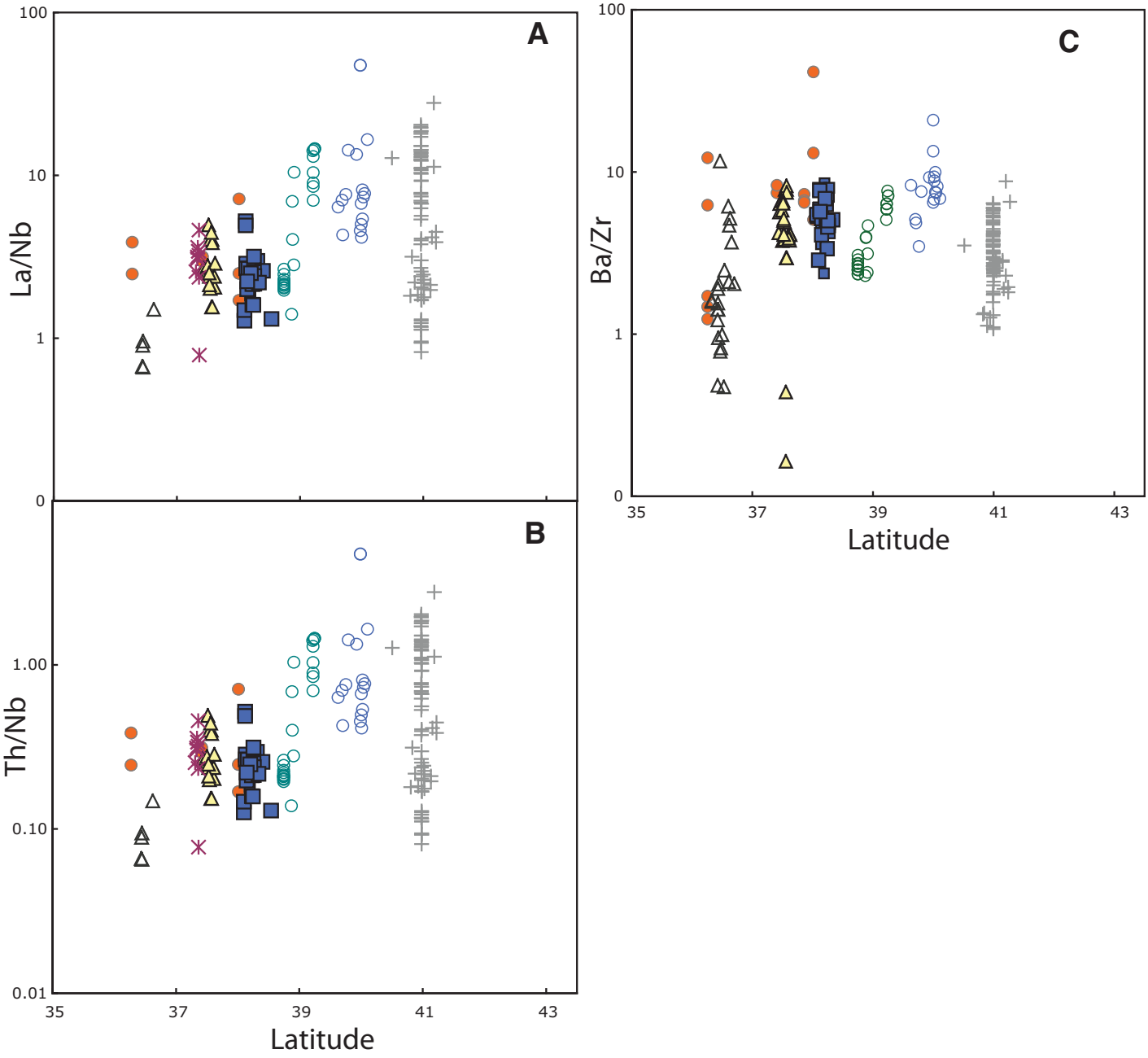

Figure 8. (A) Latitude (°N) versus La/Nb. (B) Latitude versus Th/Nb. (C) Latitude versus Ba/Zr. Symbols as in Figure 2. Each of these ratios is indicative of subduction-related, fluid-mediated inputs into the mantle wedge or mantle lithosphere. Volcanic rocks yield lower La/Nb and Th/Nb ratios from north to south, but equivalent Ba/Zr, indicating that the mantle lithosphere source south of the central Sierra Nevada contains either equal or lesser fluid-mediated enrichments compared to mantle asthenosphere to the north.

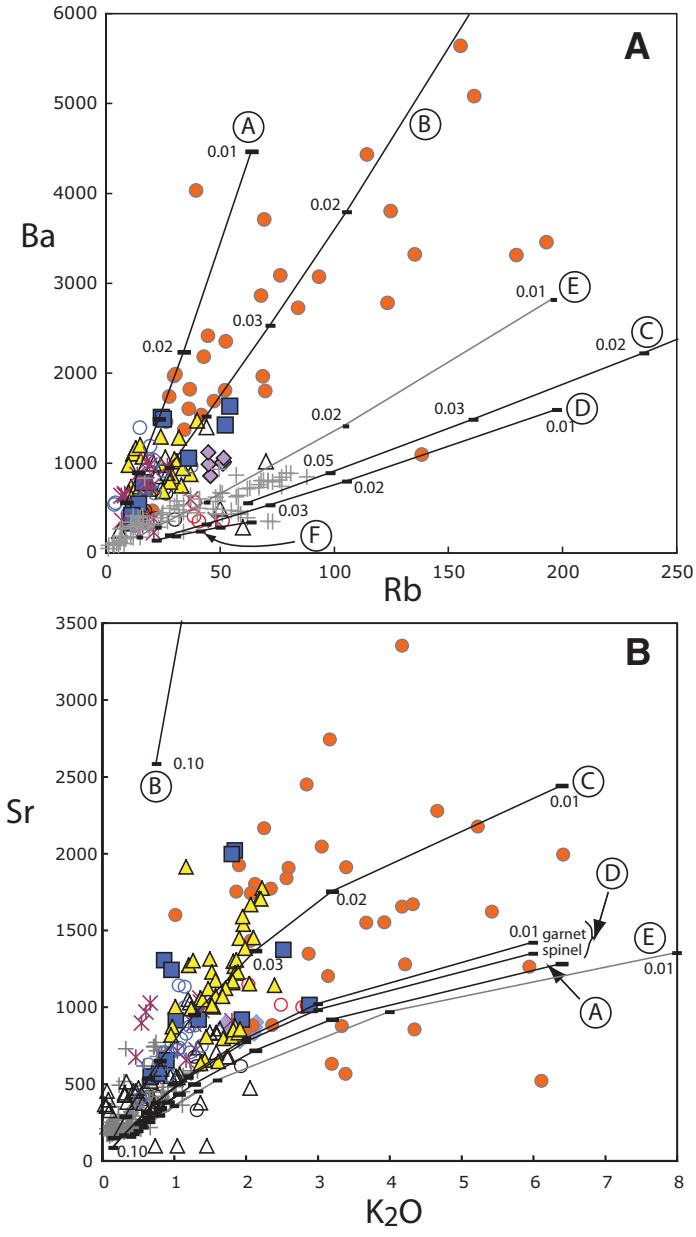

Figure 9. (A) Ba versus Rb. (B) Sr versus K_2O. Symbols as in Figure 2. Partial melting models use different Cordilleran peridotite xenoliths (Lee, 2005; Lee et al., 2006) as mantle sources (xenolith sample numbers are in parentheses): curve A (Ki5–8B), B (CP104), C (BC98–2), D (mean Sierra peridotite xenolith), E (BC76/BC52 with a garnet pyroxenite mineralogy, 30% garnet, 70% clinopyroxene), F (mean Sierra peridotite xenolith). Because we use natural rock concentrations, which are not in equilibrium with the mantle, actual mantle partial melts will have lower concentrations of Ba, Rb, Sr, and K_2O; for 100% olivine addition, dilution factors average 0.97 for rocks with 8% MgO, and 0.90 for rocks with 6% MgO. Besides E, in each case the source is a garnet peridotite, as in PM2 (Fig. 7), except for curve D, which uses both PM2 and a source with 58% olivine, 14% clinopyroxene, 26% orthopyroxene, and 2% spinel, and curve F, which is as in PM2, but with 1% phlogopite, at the expense of olivine.

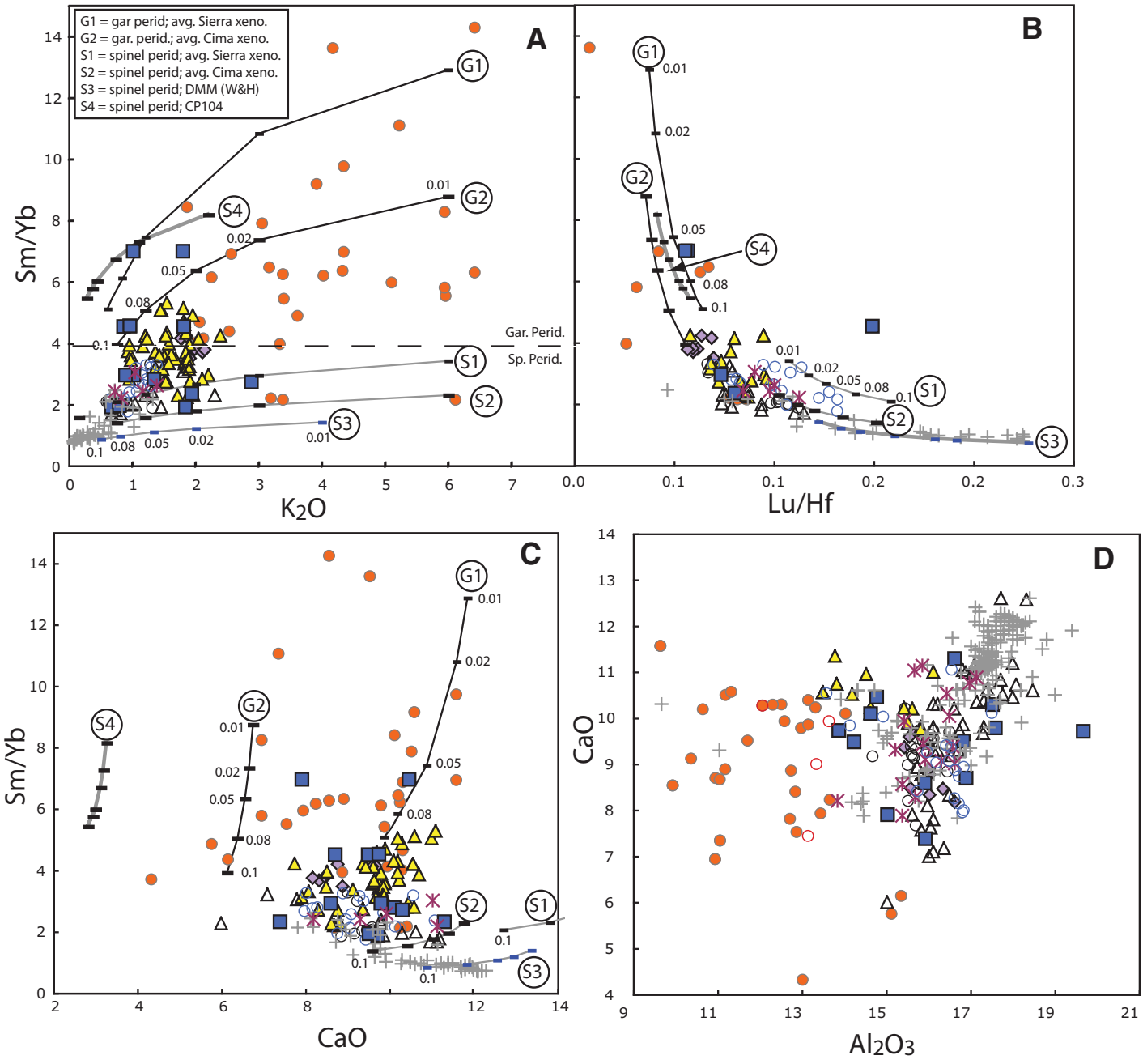

Figure 10. Peridotite partial melts in the garnet (gar; curves G) and spinel (curves S) stability fields are compared to natural samples with >8% MgO, or >10% MgO in the southern Sierra. Symbols as in Figure 2. (A) Sm/Yb versus K_2O. (B) Sm/Yb versus Lu/Hf. (C) Sm/Yb versus CaO. (D) CaO versus Al_2O_3. Bulk compositions: mean Sierran xenolith composition (curves 1), mean of xenolith compositions from Cima (curves 2), depleted mid-oceanic ridge basalt mantle, or DMM (curve 3 uses Workman and Hart, 2005), and a highly trace element–enriched but infertile peridotite xenolith from the Colorado Plateau, CP104 (curve 4). All xenolith compositions are from Lee (2005). Garnet peridotite partial melting is as in model PM2, Figure 7. Sm/Yb and Lu/Hf both indicate derivation of Pliocene high K_2O volcanics in the southern Sierra from a garnet-bearing peridotite source. C and D show that nonfertile sources from the Colorado Plateau, with very low Yb and Lu, cannot explain Sm/Yb and Lu/Hf ratios for high K_2O Pliocene volcanics since such rocks do not have major element characteristics of an ultradepleted source.

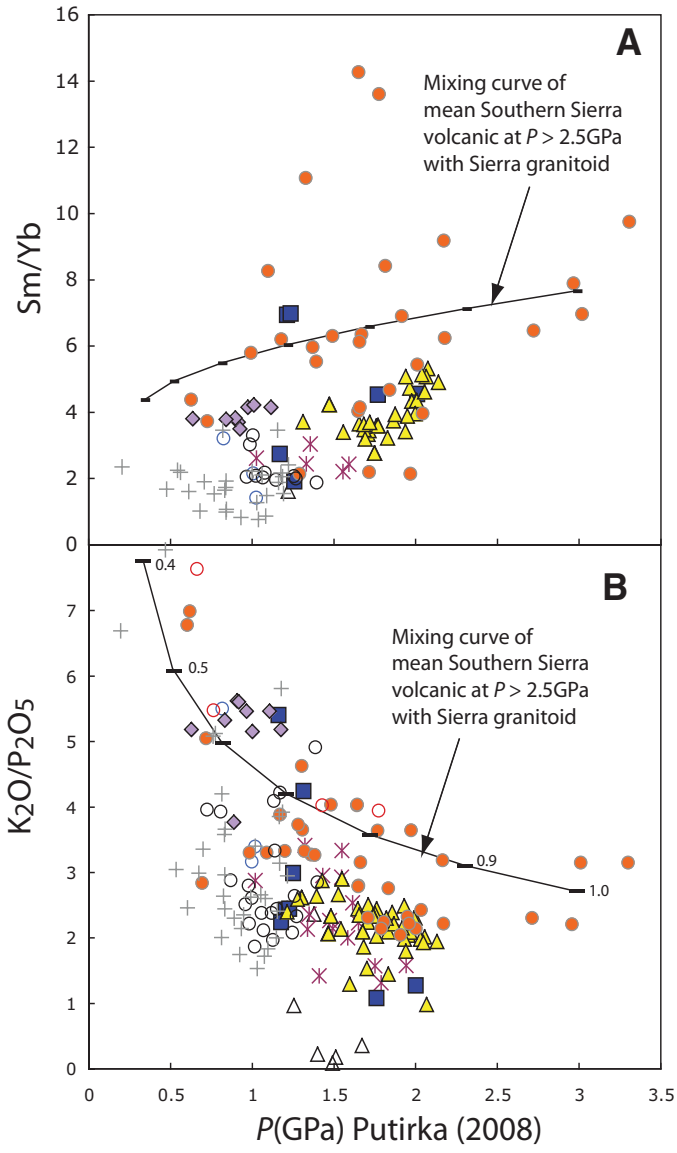

Figure 11. Symbols as in Figure 2. (A) Pressure (*P*) estimates from Putirka (2008) (see Fig. 3A) are compared to Sm/Yb and K_2O/P_2O_5. Sm/Yb is a proxy for partial melting depths, since partial melts produced in the garnet stability field of peridotite will yield much higher Sm/Yb ratios than melts produced in the spinel peridotite stability field. Some rocks with high Sm/Yb yield low *P* estimates; *P* may be lowered by AFC processes. (B) As a test, comparison is made of *P* versus an index of crust assimilation, K_2O/P_2O_5. The Sierra-wide variations in K_2O/P_2O_5 almost certainly reflect source variations in this ratio, since most Sierra samples lack evidence for high degrees of assimilation. But the southern Sierra samples show internal variation of *P* versus K_2O/P_2O_5, indicating that these rocks are affected by assimilation, and that calculated *P* values at K_2O/P_2O_5 > 3.5 are likely too low. In contrast, Sm/Yb ratios decrease slightly with AFC curves (curve 4 from Fig. 6) or not at all if assimilation rates are low (Fig. 6F), and so measured Sm/Yb ratios yield minimum estimates of partial melting depths. AFC curve 4 (from Fig. 6) is shown in each panel, where hachure marks denote residual F.

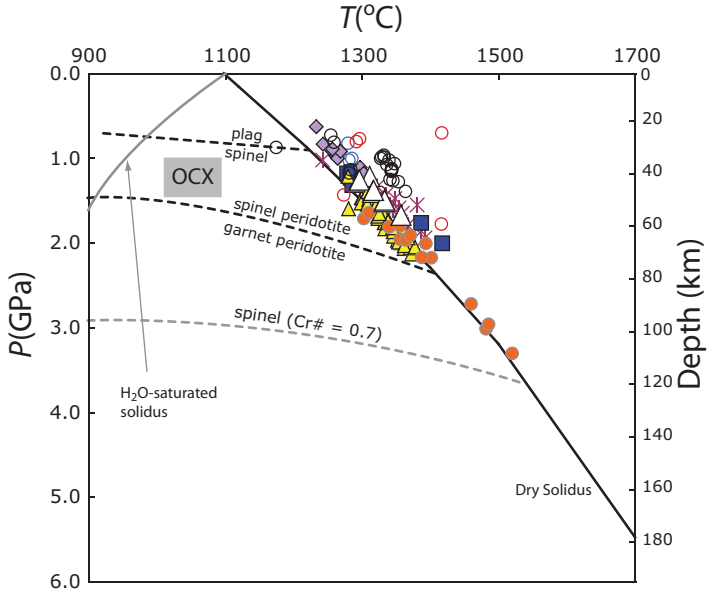

Figure 12. Pressure and temperature (*P*, *T*) estimates (see Figs. 3A, 3B; Putirka, 2008) are compared for Sierran volcanic rocks. The dry mantle solidus is from Putirka et al. (2007). The wet mantle solidus is: $T(°C) = -1.8532P^3 + 31.351P^2 - 168.52P + 1098$, where *P* is in GPa, which is effectively the wet solidus of Till et al. (2010), but recalibrated to yield the 1098 °C intercept (at 0 GPa) of the dry solidus of Putirka et al. (2007). OCX represents Oak Creek xenoliths (Lee et al., 2001); plag is plagioclase; symbols as in Figure 2. Boundaries for spinel peridotite and garnet peridotite fields are from Lee et al. (2001).

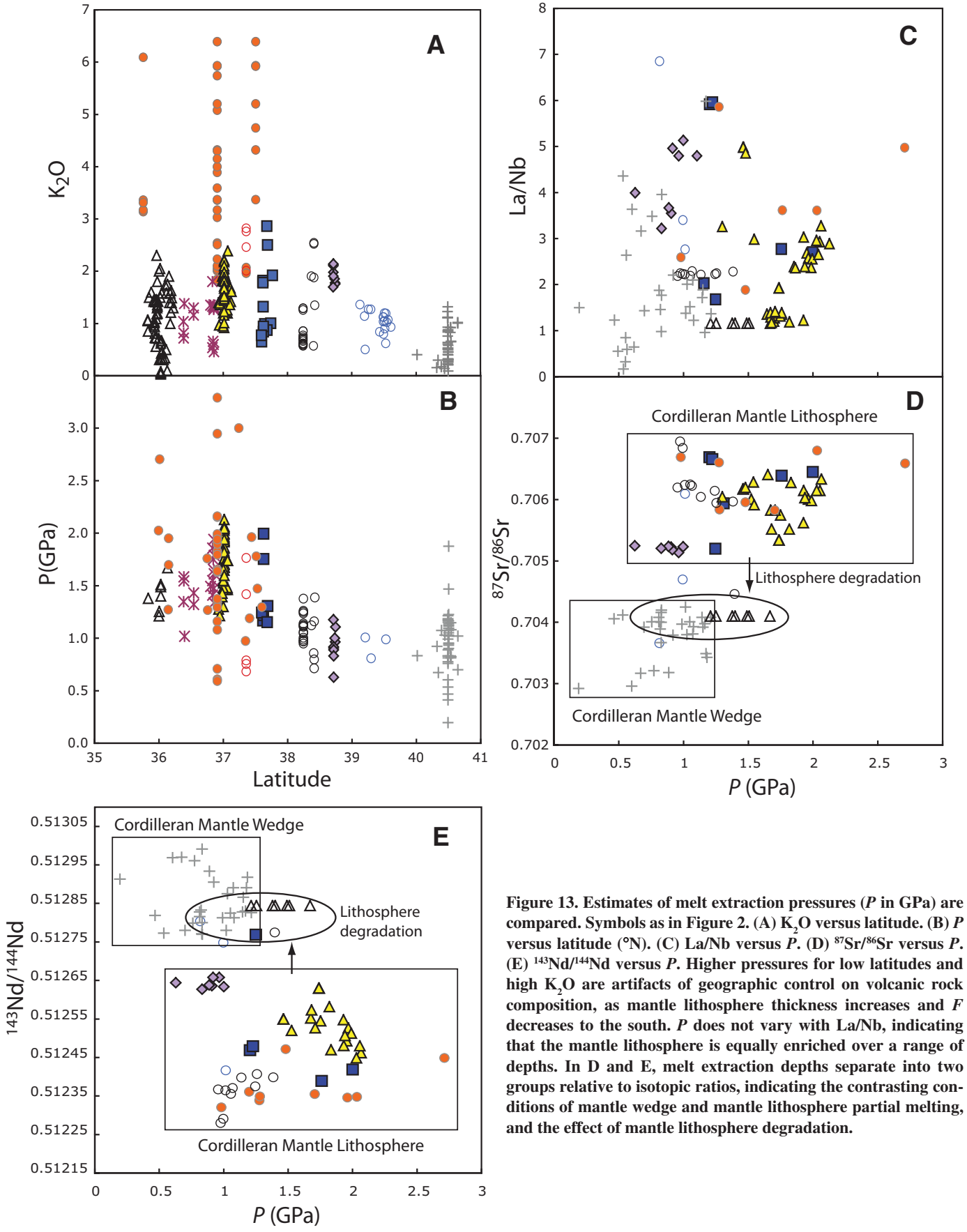

Figure 13. Estimates of melt extraction pressures (*P* in GPa) are compared. Symbols as in Figure 2. (A) K_2O versus latitude. (B) *P* versus latitude (°N). (C) La/Nb versus *P*. (D) $^{87}Sr/^{86}Sr$ versus *P*. (E) $^{143}Nd/^{144}Nd$ versus *P*. Higher pressures for low latitudes and high K_2O are artifacts of geographic control on volcanic rock composition, as mantle lithosphere thickness increases and *F* decreases to the south. *P* does not vary with La/Nb, indicating that the mantle lithosphere is equally enriched over a range of depths. In D and E, melt extraction depths separate into two groups relative to isotopic ratios, indicating the contrasting conditions of mantle wedge and mantle lithosphere partial melting, and the effect of mantle lithosphere degradation.

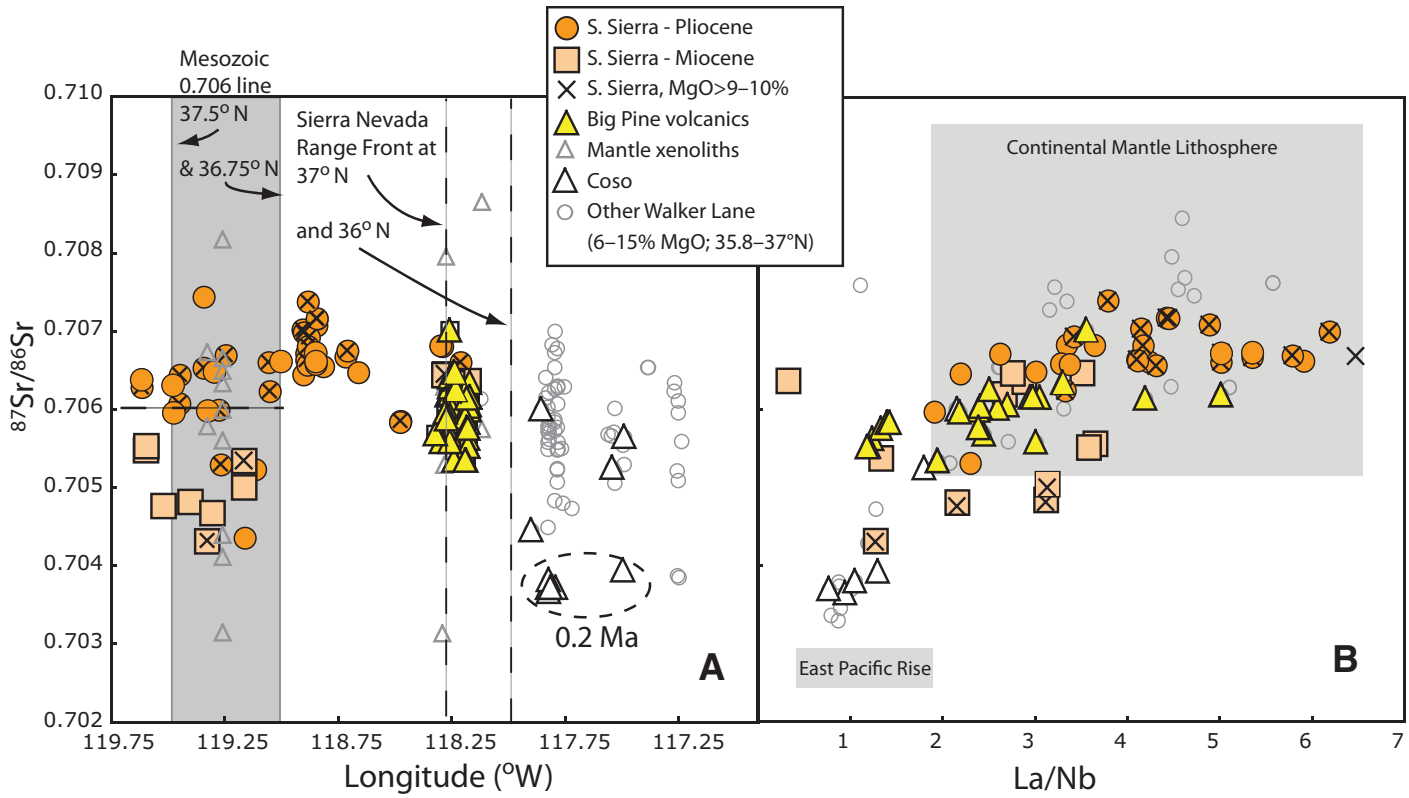

Figure 14 (*on this and following page*). (A) $^{87}Sr/^{86}Sr$ ratios are compared to longitude for Sierran and California Walker Lane volcanics (see Table 1), between 35.8°N and 37.0°N. Mantle xenoliths are from Mukhopadhyay and Manton (1994), Beard and Glazner (1995), and Ducea and Saleeby (1998a); gray field indicates Mesozoic 0.706 line for latitudes that encompass 90% of southern (S.) Sierra samples shown. Vertical dashed lines show position of Sierran range front. The $^{87}Sr/^{86}Sr$ ratios describe the same 0.706 line as do Mesozoic granitoids, and indicate that enriched mantle must still be present as far east as the range front (vertical dashed lines). Farther east, $^{87}Sr/^{86}Sr$ drops to nearly asthenosphere-like values at Coso. (B) The $^{87}Sr/^{86}Sr$ ratios are compared to La/Nb for rocks in A, which differentiates asthenosphere (East Pacific Rise; Hays, 2004) from CML (continental mantle lithosphere; DePaolo and Daley, 2000) sources.

melts into overlying CML, which would in turn explain xenolith heating and/or cooling systematics observed by Lee et al. (2001).

Space-Time Patterns

Some key questions are, where and when is CML degraded, and what triggers the process? Latitudinal sections across the Sierra Nevada (Figs. 14 and 15) and Equation 1 provide clues. In the westernmost part of the southern Sierra, the $(^{87}Sr/^{86}Sr)_i$ 0.706 line plots in the same region as does the 0.706 line of Mesozoic granitoids, as recognized by Kistler and Peterman (1973). This coincidence supports the idea that cratonic North American mantle lithosphere underlies regions where $(^{87}Sr/^{86}Sr)_i > 0.706$ (Kistler, 1990). However, while Mesozoic rocks retain high $(^{87}Sr/^{86}Sr)_i$ to the east (Kistler, 1990), $^{87}Sr/^{86}Sr$ ratios for very young Walker Lane volcanic rocks (e.g., Coso) approach asthenosphere-like values, a result that has been attributed to extension and thinning of the mantle lithosphere, related to evolution of the MTJ (Ormerod et al., 1988). In the southern Sierra, the spatial transition is illustrated by $^{87}Sr/^{86}Sr$ ratios, which have CML-like values for Pliocene volcanics erupted within the range, but decline to moderate values for Pleistocene–Holocene Big Pine volcanics at the Sierran range front (Fig. 14A), and decline further to approach asthenosphere-like values for young volcanics at Coso (at ~117.8°W). Mantle xenoliths at Big Pine further show that CML must still exist at the range front, with $^{87}Sr/^{86}Sr$ ratios that exceed values found for Pliocene volcanics (Fig. 14A), and $^{143}Nd/^{144}Nd$ in host volcanics as low as 0.512194, lower than southern Sierran Pliocene lavas (which range to 0.51222).

Why do only very young Coso volcanics approach an asthenosphere composition? We use Equation 1 and data in Figure 14A to better test a model first proposed by Ormerod et al. (1988), that the evolving North American–Pacific plate boundary may control volcanic isotope compositions. In Figures 14C and 14D, 0 Ma marks the time of MTJ arrival at a given latitude, while positive values to the right of 0 Ma indicate the lag time between MTJ arrival and eruption; these times are compared to isotopic compositions. Volcanic rocks reveal movement away from asthenosphere and toward a CML source, then back toward asthenosphere. We interpret these trends to reflect partial melting of asthenosphere as it upwells to replace a sinking Farallon plate. Partial melts from the asthenosphere, or perhaps the asthenosphere itself, induce lithosphere heating, and so CML degrades over a 20 Ma time interval. Only Coso volcanics are sufficiently young (Figs. 14C, 14D) and far enough east (Fig. 14A) to be affected by maximum CML degradation, so as to yield a strong asthenosphere component.

North of 37°N, the temporal patterns for Sierran volcanics are different; there, $^{87}Sr/^{86}Sr$ ratios trend to higher values to the east regardless of age (Fig. 15A). South and east of Lassen,

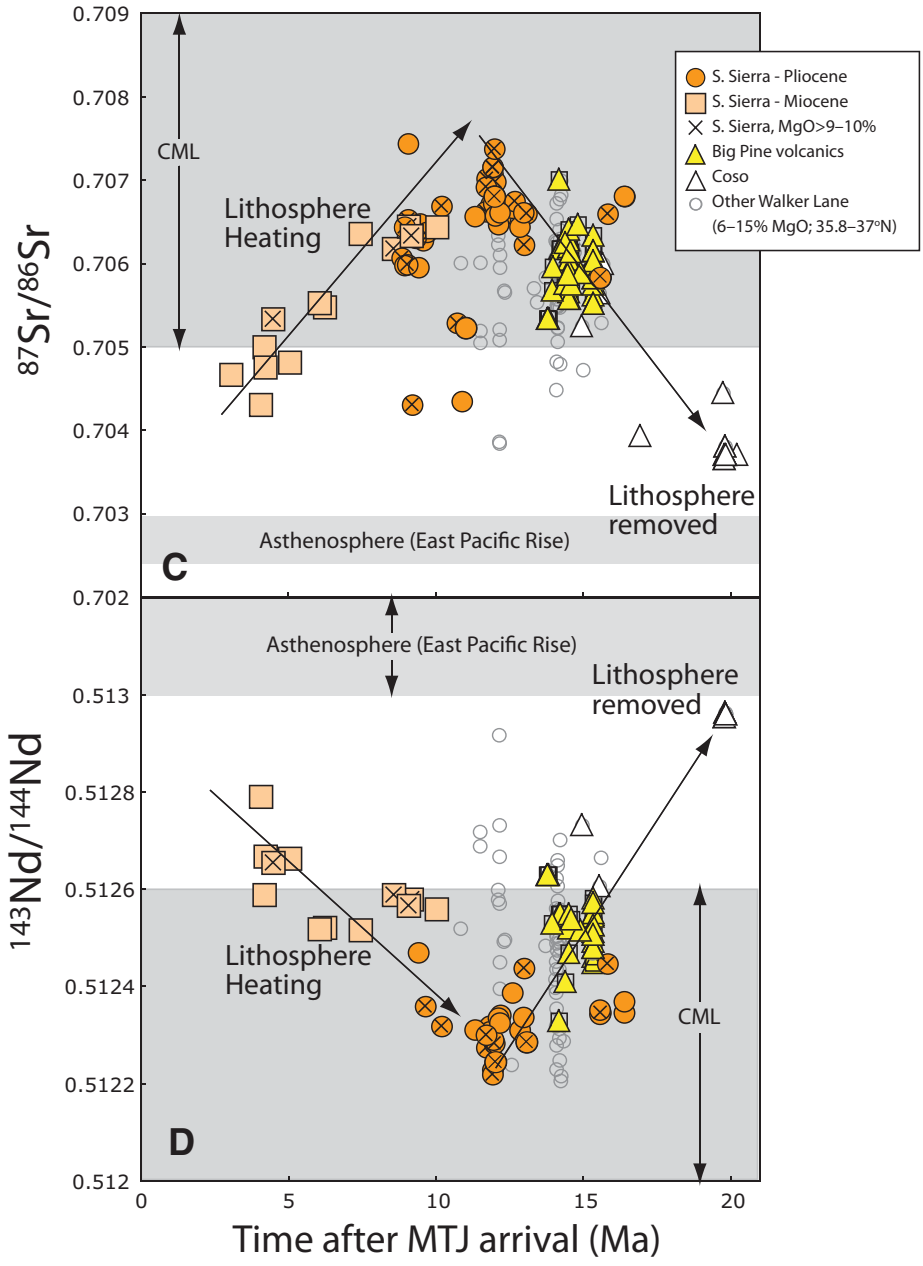

Figure 14 (*continued*). (C) The $^{87}Sr/^{86}Sr$ ratios of volcanic rocks in A are compared relative to the time of arrival of the Mendocino Triple Junction (MTJ), using Equation 1 (see text). (D) $^{143}Nd/^{144}Nd$ ratios comparison. Reconstructed latitudes are based on Snow and Wernicke (2000); most volcanics, however, are so young compared to the time extension that the correction is effectively nil. The CML isotopic range may reflect real variation within CML, or mixing between CML and asthenosphere. C and D show an early phase of lithosphere heating with increasing CML influence at 0–12 Ma, post-MTJ arrival, followed by a phase of lithosphere degradation from 15 to 20 Ma post-MTJ.

$^{87}Sr/^{86}Sr$ ratios only increase with decreasing age (Fig. 15B); this most likely indicates a still-increasing phase of CML heating. Many of these rocks erupted prior to MTJ arrival, but are probably still affected by Pacific–North American plate reorganization, as illustrated by McQuarrie and Wernicke (2005).

SUMMARY AND SYNTHESIS

Space-time-composition trends confirm some old views of, and provide some new insights into, Sierran tectonics. First, we show that Sierran Cenozoic volcanic rocks demarcate a $(^{87}Sr/^{86}Sr)_i = 0.706$ line similar to that defined by Mesozoic granitoids, a line that marks the western edge of North American CML (Kistler, 1990; Fig. 14A). Unlike Mesozoic granitoids, however, young Cenozoic volcanics in the southern Sierra transition to asthenosphere-like values to the east, in the Walker Lane (Fig. 14A). The Walker Lane is thus a region of asthenosphere upwelling and CML degradation, and both processes are triggered by MTJ arrival (Figs. 14C, 14D). Heating of the CML occurs over a span of ~12 Ma, at which point CML degrades and is nearly gone by 20 Ma, post-MTJ arrival at any given latitude (Figs. 14C, 14D). In the southern Sierra, Miocene volcanism signals slab-window opening, while Pliocene volcanism marks the culmination of CML heating; Coso and Big Pine volcanics mark steps toward nearly complete CML removal, as lithosphere degradation encroaches upon the Sierra Nevada (Fig. 14A). North of 37°N, in contrast, asthenosphere upwelling in the Walker Lane is too recent to allow complete CML removal. There, only a CML heating phase is evident (Fig. 15B), which is affected not just by a north-migrating MTJ, but also by a west-propagating ancestral Cascades arc (Colgan et al., 2011; Busby and Putirka, 2009).

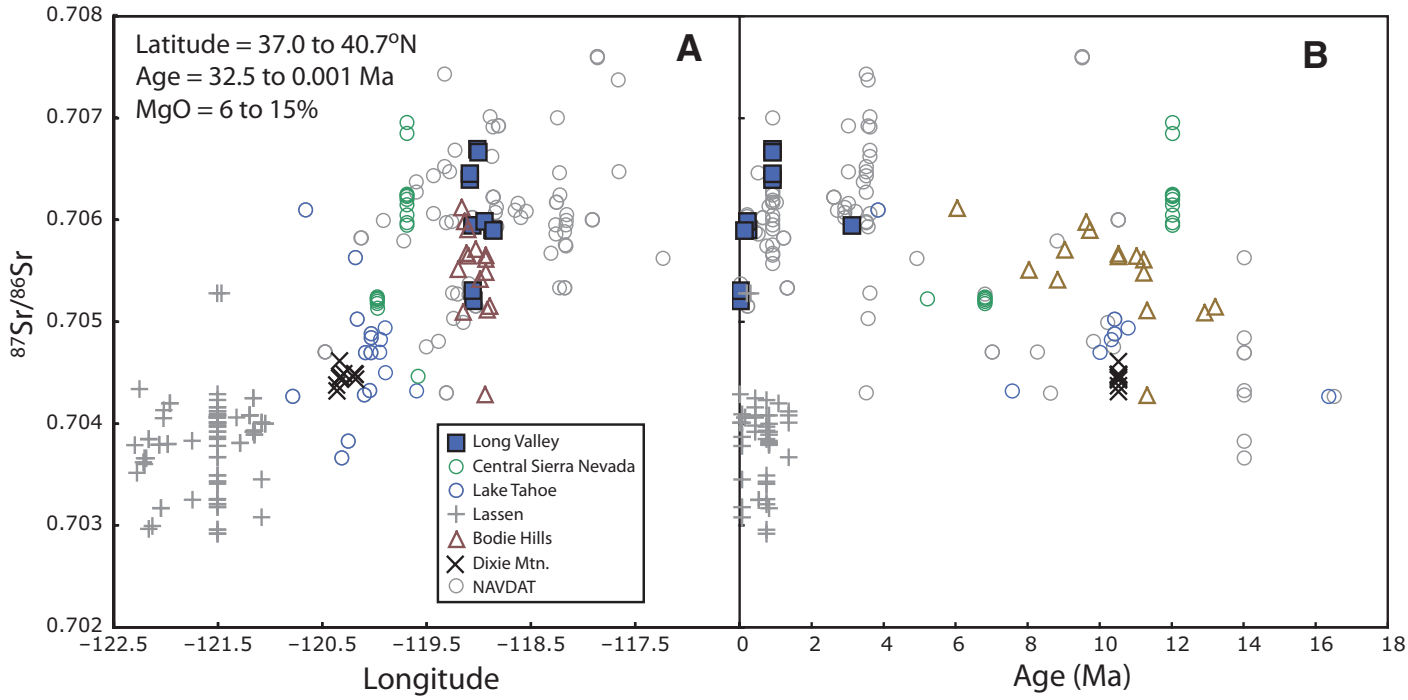

Figure 15. $^{87}Sr/^{86}Sr$ ratios for Sierran and California Walker Lane volcanic rocks erupted between 37.0°N and 40.7°N (Table 1). (A) Compared to longitude (NAVDAT—North American Volcanic and Intrusive Rock Database; www.navdat.org. (B) Compared to age. Unlike Figure 14, no temporal trend toward an asthenosphere source beneath the Walker Lane belt is evident north of 37°N. Instead, asthenosphere (mantle wedge) partial melting occurs to the west, beneath Lassen, while the temporal trend in B indicates lithosphere heating, rather than lithosphere degradation (cf. Fig. 14C). Although the Walker Lane is a region of extension, lithosphere degradation and removal are incomplete and still in progress.

Silicate melt barometry reveals the depth extent of Sierran CML, which extends from the base of the crust (40 km) to ~75 km beneath most of the range, and to ~110 km beneath the southern Sierra, at least in the Pliocene. CML thus must still be partially intact to depths of 75 km beneath most of the Sierra Nevada, from 35°N to 39°N. These results conflict with conclusions drawn by some seismic studies, which state or imply that Sierran crust directly overlies asthenosphere (Fliedner and Ruppert, 1996; Savage et al., 2003; Jones et al., 2004; Frassetto et al., 2011), but are consistent with those of Li et al. (2007), who indicated a 70-km-thick mantle lithosphere beneath the range front, and Ormerod et al. (1988) and DePaolo and Daley (2000), who illustrated comparable spatial patterns of lithosphere removal.

To reconcile geochemical and seismic observations, we present a new model of lithosphere degradation (Fig. 16A) adapted from Zandt et al. (2004), Li et al. (2007), and Frassetto et al. (2011). We posit that asthenosphere upwells with arrival of the MTJ and opening of a slab window (Fig. 16B) (Atwater, 1970; Atwater and Stock, 1998). This initiates asthenosphere partial melting, and these partial melts, and perhaps the asthenosphere, invade CML (Figs. 14C, 14D), which then degrades (Fig. 16A) (J. Saleeby, 2011, personal commun.). In the central Sierra, the situation is more complex: there, MTJ arrival is preceded by a southwest-migrating arc of volcanism, which culminates in the formation of the ancestral Cascades (Busby and Putirka, 2009; Colgan et al. 2011). The merging of these tectonic spatial trends is observed in the central Sierra, where ancestral Cascade volcanism begins at 16 Ma and is interrupted by a burst of high K_2O volcanism at 10 Ma. The high K_2O volcanics (latites) emanate from transtensional faults near the modern range front, and signal the birth of the Sierra Nevada microplate there (Busby and Putirka, 2009), but still carry a CML isotopic signature. Such transtensional stresses characterize the Walker Lane (Bursik, 2009; Muffler et al., 2008), where most pulses of high K_2O volcanism likely mark episodes of transtensional strain (Putirka and Busby, 2007; Busby and Putirka, 2009), not lithosphere degradation.

This new model is not necessarily in conflict with prior work on Sierran mantle xenoliths or seismic studies. Our model allows for the loss of garnet-bearing lowermost lithosphere (>70 km depths; Fig. 12) beneath the eastern Sierra (Ducea and Saleeby, 1996), and garnet-bearing crust can be lost by lateral mass transfer (Bird, 1991; Zandt et al., 2004; Le Pourhiet et al., 2006). DePaolo and Daley (2000), for example, estimated initial lithosphere thicknesses of 100 km, comparable to our estimates beneath Pliocene Sierran rocks, but 25–30 km less than our estimates for lithosphere thicknesses at the range front. Since garnet is stable only below 70–75 km, our projected loss of CML is sufficient to eliminate garnet-bearing peridotite (Fig. 12). As to observed P- and S-wave velocities, low velocities may reflect the retention of small amounts of melt in a degrading CML, the presence of which can have a profound impact on seismic signals (Hammond and Humphreys, 2000). Our model also appears to be consistent with the Schmandt and Humphreys (2010, fig. 12 therein) imaging of transitional-velocity mantle beneath the range front, and is in excellent agreement with the Li et al. (2007) 70 km estimate for lithosphere thickness and the Ito and Simons (2011) estimate that asthenosphere lies between 80 and 220 km beneath California.

If asthenosphere and mantle lithosphere sources intermix, volcanic rocks should plot on

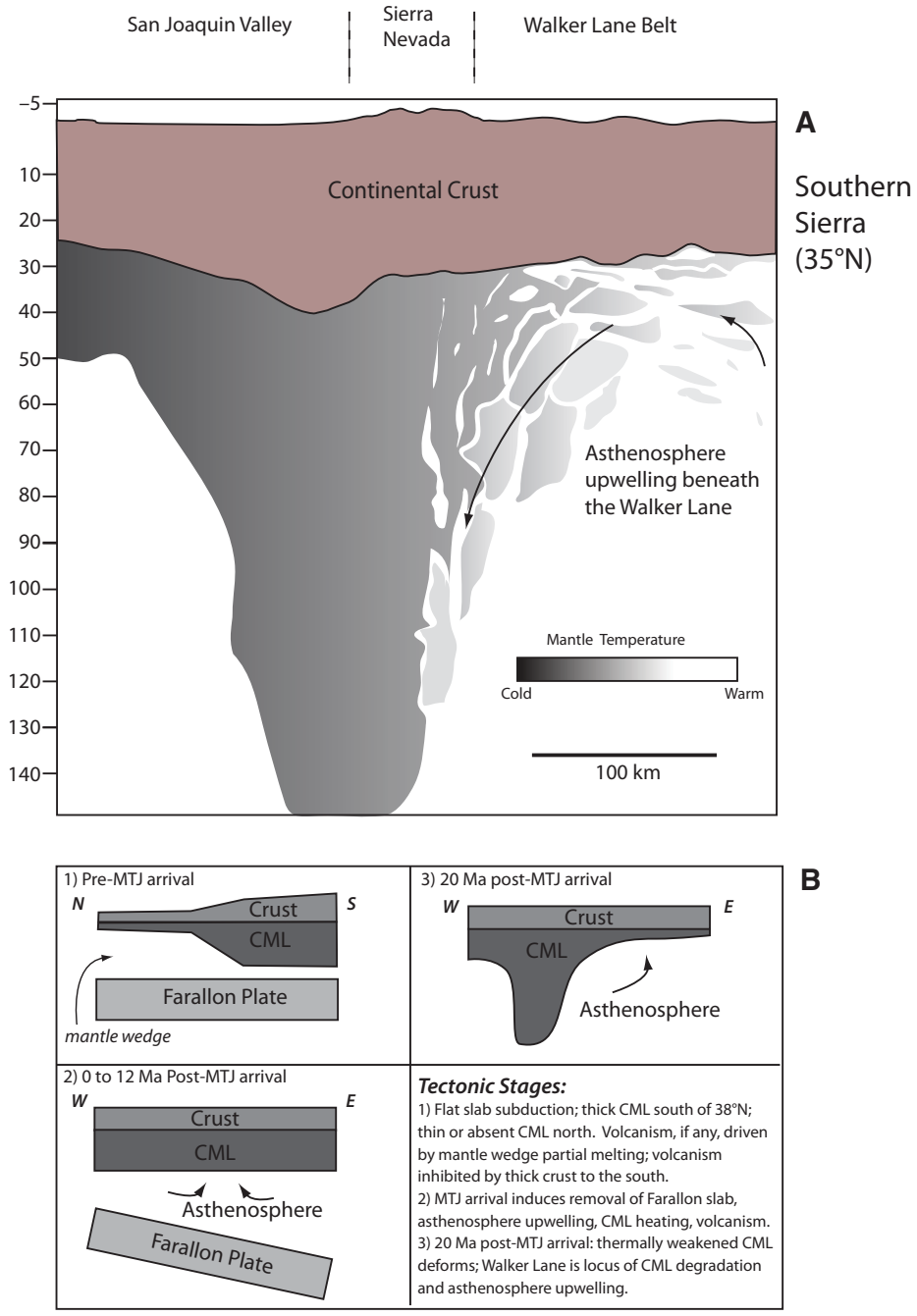

Figure 16. A new model of mantle lithosphere degradation. (A) A hypothetical profile across the southern Sierra into the Walker Lane. Crustal thicknesses are based on Fliedner and Ruppert (1996; although we remove the crustal keel beneath the range front, which does not appear in other seismic cross sections); mantle cross-section thicknesses are based on Li et al. (2007), Zandt et al. (2004), and Frassetto et al. (2011). Continental crust is in brown and mantle lithosphere is in shades of gray; light colors indicate hotter lithosphere, or asthenosphere. We expect that cold lithosphere may grade imperceptibly into asthenosphere. In the southern Walker Lane, the process of CML (continental mantle lithosphere) degradation is nearly complete, but is just underway at the Sierra range front, as mantle upwelling encroaches upon the range. (B) An evolutionary path relative to the arrival of the Mendocino Triple Junction (MTJ) at any given latitude; A represents a detailed model for stage 3 shown in B.

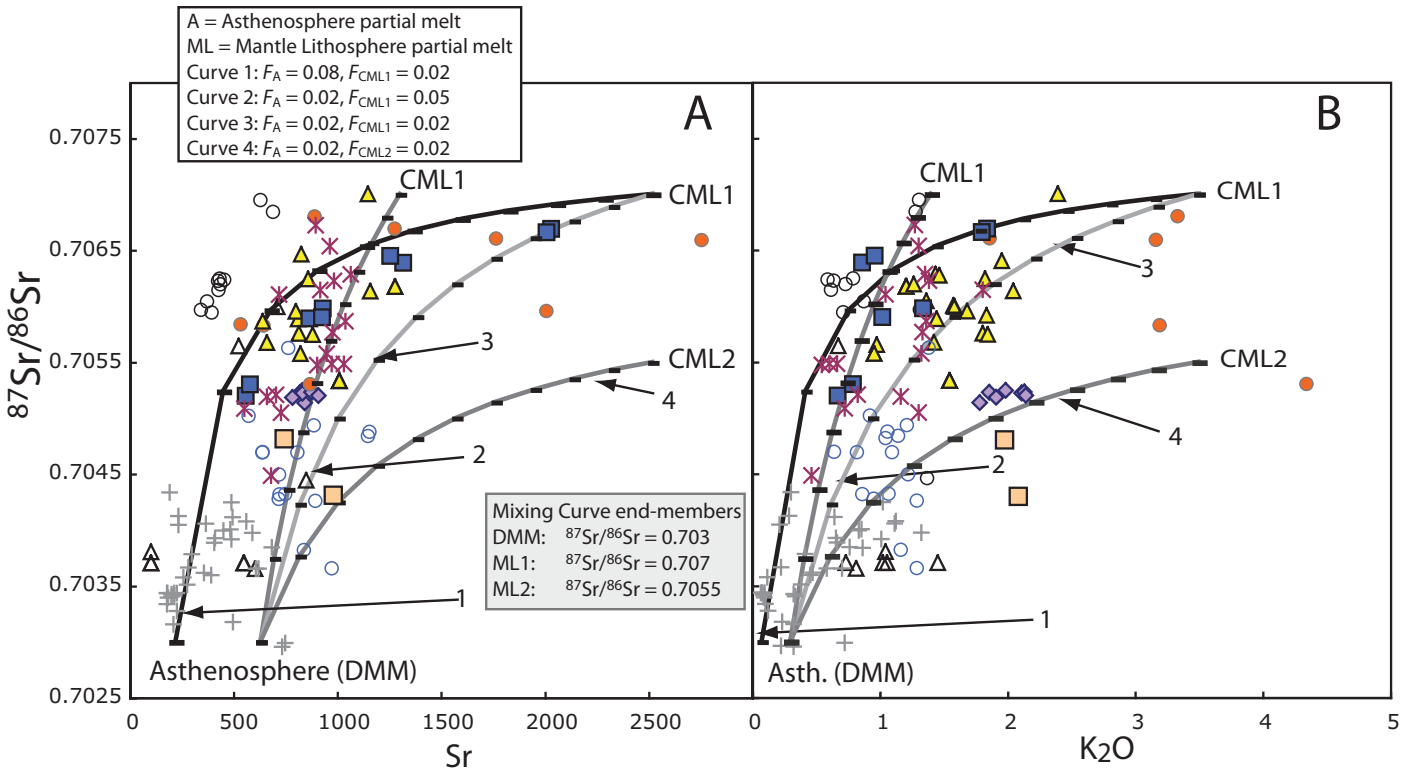

Figure 17. (A) $^{87}Sr/^{86}Sr$ compared to Sr. DMM—depleted mid-oceanic ridge basalt mantle. (B) $^{87}Sr/^{86}Sr$ compared to K_2O. Symbols as in Figure 2. F_A, F_{CML1}, and F_{CML2} are melt fractions of mantle partial melts from asthenosphere ($^{87}Sr/^{86}Sr$ = 0.703, Sr = 20 ppm, K_2O = 0.006 wt%; Workman and Hart, 2005) and two mantle lithosphere sources, CML1 (CML—continental mantle lithosphere) ($^{87}Sr/^{86}Sr$ = 0.707, Sr = 80 ppm, K_2O = 0.07 wt%; Beard and Glazner, 1995; Lee, 2005) and CML2 ($^{87}Sr/^{86}Sr$ = 0.7055, Sr = 80 ppm, K_2O = 0.07 wt%). Regardless of whether mantle lithosphere (CML1 and CML2) is more fertile (curve 1), equally fertile (curves 3 and 4), or less fertile (curve 2) than asthenosphere (A), the Sierran intersuite trend is consistent with mixing between partial melts generated between an enriched (CML) and a depleted (asthenosphere) source; most likely both the mantle lithosphere and asthenosphere sources are more heterogeneous than indicated here. For example, Coso $^{87}Sr/^{86}Sr$-K_2O relationships are better described by mixing between a source with $^{87}Sr/^{86}Sr$ = 0.704 (not shown).

a mixing curve between partial melts generated from both sources. To illustrate, we compare $^{87}Sr/^{86}Sr$ to Sr and K_2O concentrations (Fig. 17). At least three mantle components appear to be required; an asthenosphere component (DMM, depleted mid-oceanic ridge basalt mantle; Workman and Hart, 2005; $^{87}Sr/^{86}Sr$ = 0.703, Sr = 20 ppm, K_2O = 0.006 wt %), and two CML sources: CML1, with $^{87}Sr/^{86}Sr$ = 0.707 (Sr = 80 ppm, K_2O = 0.07 wt%; see Beard and Glazner, 1995; Lee, 2005), and CML2, with $^{87}Sr/^{86}Sr$ = 0.7055. This range suggests that the widths of the CML fields in Figures 14C and 14D (from DePaolo and Daley, 2000) are real, rather than a product of mixing between a singular CML source and asthenosphere. For completeness, our models assume higher, equal, and lower degrees of partial melting in the CML sources compared to DMM, since CML may be equally fertile as, or more fertile than, DMM; but to explain the heating observed by Lee et al. (2001), we expect that $T_{DMM} > T_{CML}$. In addition, Coso volcanics are clearly not derived from pure or unmodified asthenosphere (Figs. 14C, 14D, and 17); Coso is only explained if its source contains 0.02 wt% K_2O (compared to 0.006% K_2O in DMM; Workman and Hart, 2005). Regardless of the precise components or means of mixing, a new view of mantle degradation is needed, and that provided by Figure 16 might be useful for simultaneously explaining seismic and geochemical observations.

ACKNOWLEDGMENTS

We thank Cathy Busby and her students, Jeanette Hagan, Alice Koerner, and Ben Melosh, for their field work, which has been key to our interpretation of the tectonic significance of Cenozoic volcanism in the Sierra Nevada. We also thank the students of EES 101 Igneous and Metamorphic Petrology classes of 2003–2004, for their participation in this project. Putirka greatly appreciated discussions with George Zandt, whose comments helped to inspire the model presented in Figure 16. We also appreciate reviews of early drafts of this manuscript by Jason Saleeby, Cin-Ty Lee, and Lang Farmer, and Jason's allowing us to view an advance copy of a paper in review. The final manuscript was greatly improved by thoughtful reviews by Yildrim Dilek, Lang Farmer, and Cathy Busby. This research was supported by National Science Foundation grants EAR-0711276 and EAR-0711150 (to Putirka and Busby), EAR-0421272, and EAR-0313688 (to Putirka).

REFERENCES CITED

Agee, C.B., and Draper, D.S., 2004, Experimental constraints on the origin of Martian meteorites and the composition of the Martian mantle: Earth and Planetary Science Letters, v. 224, p. 415–429, doi: 10.1016/j.epsl.2004.05.022.

Anderson, A.T., and Gottfried, D., 1971, Contrasting behavior of P, Ti, and Nb in a differentiated high-alumina olivine tholeiite and calc-alkaline andesite suite: Geological Society of America Bulletin, v. 82, p. 1929–1942, doi: 10.1130/0016-7606(1971)82[1929:CBOPTA]2.0.CO;2.

Atwater, T., 1970, Implications of plate tectonics for the Cenozoic tectonic evolution of western North America: Geological Society of America Bulletin, v. 81, p. 3513–3536, doi: 10.1130/0016-7606(1970)81[3513:IOPTFT]2.0.CO;2.

Atwater, T., and Stock, J., 1998, Pacific–North America plate tectonics of the Neogene southwestern United States—An update: International Geology Review, v. 40, p. 375–402, doi: 10.1080/00206819809465216.

Babcock, J.W., 1977, The late Cenozoic Coso volcanic field, Inyo County, California [Ph.D. thesis]: Santa Barbara, University of California, 213 p.

Bacon, C.R., MacDonald, R., Smith, R.L., and Baedecker, P.A., 1981, Pleistocene high-silica rhyolites of the Coso volcanic field, Inyo County, California: Journal of Geophysical Research, v. 86, p. 10223–10241, doi: 10.1029/JB086iB11p10223.

Bacon, C.R., Kurasawa, H., Delevaux, M., Kistler, R.W., and Doe, B.R., 1984, Lead and strontium isotopic evidence for crustal interaction and compositional zonation in the source regions of Pleistocene basaltic and rhyolitic magmas of the Coso volcanic field, California: Contributions to Mineralogy and Petrology, v. 85, p. 366–375, doi: 10.1007/BF01150293.

Bailey, R.A., 2004, Eruptive history and chemical evolution of the precaldera and postcaldera basalt-dacite sequences, Long Valley, California: Implications for magma sources, current seismic unrest and future volcanism: U.S. Geological Survey Professional Paper P-1692, 75 p.

Baker, M.B., Grove, T.L., and Price, R.C., 1994, Primitive basalts and andesites from the Mt. Shasta region, N. California: Products of varying melt fraction and water content: Contributions to Mineralogy and Petrology, v. 118, p. 111–129, doi: 10.1007/BF01052863.

Bartels, K.S., Kinzler, R.J., and Grove, T.L., 1991, High pressure phase relations of primitive high-alumina basalts from Medicine Lake volcano, northern California: Contributions to Mineralogy and Petrology, v. 108, p. 253–270, doi: 10.1007/BF00285935.

Beard, B.L., and Glazner, A.F., 1995, Trace element and Sr and Nd isotopic composition of xenoliths from the Big Pine volcanic field, California: Journal of Geophysical Research, v. 100, p. 4169–4179, doi: 10.1029/94JB02883.

Beard, B.L., and Glazner, A.F., 1998, Petrogenesis of isotopically unusual Pliocene olivine leucitites from Deep Springs Valley, California: Contributions to Mineralogy and Petrology, v. 133, p. 402–417, doi: 10.1007/s004100050462.

Beard, B.L., and Johnson, C.M., 1997, Hafnium isotope evidence for the origin of Cenozoic basaltic lavas from the southwestern United States: Journal of Geophysical Research, v. 102, p. 20149–20178, doi: 10.1029/97JB01731.

Bird, P., 1991, Lateral extrusion of lower crust from under high topography, in the isostatic limit: Journal of Geophysical Research, v. 96, p. 10275–10286, doi: 10.1029/91JB00370.

Bohrson, W.A., and Spera, F.J., 2001, Energy-constrained open system magmatic processes II: Application of energy-constrained assimilation-fractional crystallization (EC-AFC) model to magmatic systems: Journal of Petrology, v. 42, p. 1019–1041, doi: 10.1093/petrology/42.5.1019.

Blatter, D.W., and Carmichael, I.S.E., 2001, Hydrous phase equilibria of a Mexican high-silica andesite: A candidate for a mantle origin: Geochimica et Cosmochimica Acta, v. 65, p. 4043–4065, doi: 10.1016/S0016-7037(01)00708-6.

Blondes, M.S., Reiners, P.W., Ducea, M.N., Singer, B.S., and Chesley, J., 2008, Temporal-compositional trends over short and long time scales in basalts of the Big Pine volcanic field, California: Earth and Planetary Science Letters, v. 269, p. 140–154, doi: 10.1016/j.epsl.2008.02.012.

Borg, L.E., and Clynne, M.A., 1998, The petrogenesis of felsic calc-alkaline magmas from the southernmost Cascades, California: Origin by partial melting of basaltic lower crust: Journal of Petrology, v. 39, p. 1197–1222, doi: 10.1093/petrology/39.6.1197.

Bradshaw, T.K., Hawkesworth, C.J., and Gallagher, K., 1993, Basaltic volcanism in the southern Bain and Range: No role for a mantle plume: Earth and Planetary Science Letters, v. 116, p. 45–62, doi: 10.1016/0012-821X(93)90044-A.

Bulatov, V.K., Girnis, A.V., and Brey, G.P., 2002, Experimental melting of a modally heterogeneous mantle: Mineralogy and Petrology, v. 75, p. 131–152, doi: 10.1007/s007100200021.

Bullen, T.D., and Clynne, M.A., 1990, Trace element and isotopic constrains on magmatic evolution at Lassen Volcanic Center: Journal of Geophysical Research, v. 95, p. 19671–19691, doi: 10.1029/JB095iB12p19671.

Bursik, M., 2009, A general model of tectonic control of magmatism: Examples from Long Valley Caldera (USA) and El Chichón (Mexico): Geofísica Internacional, v. 48, p. 171–183.

Busby, C.J., and Putirka, K., 2009, Cretaceous-Cenozoic landscape evolution of the SW USA: Evidence from Cenozoic paleocanyon fill in the central Sierra Nevada: International Geology Review, v. 51, p. 670–701, doi: 10.1080/00206810902978265.

Busby, C.J., DeOreo, S.B., Skilling, I., Gans, P.B., and Hagan, J.C., 2008a, Carson Pass–Kirkwood paleocanyon system: Paleogeography of the ancestral Cascades arc and implications for landscape evolution of the Sierra Nevada (California): Geological Society of America Bulletin, v. 120, p. 274–299, doi: 10.1130/B25849.1.

Busby, C.J., Hagan, J.C., Putirka, K., Pluhar, C.J., Gans, P., Wagner, D.L., Rood, D., DeOreo, S.B., and Skilling, I., 2008b, The ancestral Cascades arc: Cenozoic evolution of the central Sierra Nevada (California) and the birth of the new plate boundary, *in* Wright, J.E., and Shervais, J.W., eds., Ophiolites, Arcs, and Batholiths: A Tribute to Cliff Hopson: Geological Society of America Special Paper 438, p. 331–378, doi: 10.1130/2008.2438(12).

Carmichael, I.S.E., Nicholls, J., and Smith, A.L., 1970, Silica activity in igneous rocks: American Mineralogist, v. 55, p. 246–263.

Colgan, J.P., Egger, A.E., John, D.A., Cousens, B., Fleck, R.J., and Henry, C.D., 2011, Oligocene and Miocene arc volcanism in northeastern California: Evidence for post-Eocene segmentation of the subducting Farallon plate: Geosphere, v. 7, p. 733–755, doi: 10.1130/GES00650.1.

Cousens, B.L., 1996, Magmatic evolution of Quaternary mafic magmas at Long Valley Caldera and the Devils Postpile, California: Effects of crustal contamination on lithospheric mantle-derived magmas: Journal of Geophysical Research, v. 101, p. 27673–27689, doi: 10.1029/96JB02093.

Cousens, B., Prytulak, J., Henry, C., Alcazar, A., and Brownrigg, T., 2008, Geology, geochronology, and geochemistry of the Miocene–Pliocene ancestral Cascades arc, northern Sierra Nevada, California and Nevada: The roles of the upper mantle, subducting slab and the Sierra Nevada lithosphere: Geosphere, v. 4, p. 829–853, doi: 10.1130/GES00166.1.

Daley, E.E., and DePaolo, D.J., 1992, Isotopic evidence for lithospheric thinning during extension: Southeastern Great Basin: Geology, v. 20, p. 104–108, doi: 10.1130/0091-7613(1992)020<0104:IEFLTD>2.3.CO;2.

Davidson, J., and Wilson, M., 2011, Differentiation and source processes at Mt Pelee and the Quill; active volcanoes in the Lesser Antilles Arc: Journal of Petrology, v. 52, p. 1493–1531, doi: 10.1093/petrology/egq095.

Davidson, J., Turner, S., Handley, H., Macpherson, C., and Dosseto, A., 2007, Amphibole "sponge" in arc crust?: Geology, v., 35, p. 787–790, doi: 10.1130/G23637A.1.

DePaolo, D.J., 1981, Trace element and isotopic effects of combined wallrock assimilation and fractional crystallization: Earth and Planetary Science Letters, v. 53, p. 189–202, doi: 10.1016/0012-821X(81)90153-9.

DePaolo, D.J., and Daley, E.E., 2000, Neodymium isotopes in basalts of the southwest Basin and Range and lithosphere thinning during continental extension: Chemical Geology, v. 169, p. 157–185, doi: 10.1016/S0009-2541(00)00261-8.

DePaolo, D.J., and Farmer, G.L., 1984, Isotopic data bearing on the origin of Mesozoic and Tertiary granitic rocks in the western United States: Royal Society of London Philosophical Transactions, ser. A, v. 310, p. 743–753, doi: 10.1098/rsta.1984.0017.

Dodge, F.C.W., and Moore, J.G., 1981, Late Cenozoic volcanic rocks of the southern Sierra Nevada, California, II: Geochemistry: Summary: Geological Society of America Bulletin, v. 92, p. 912–914, doi: 10.1130/0016-7606(1981)92<912:LCVROT>2.0.CO;2.

Donnelly-Nolan, J.M., Champion, D.E., Grove, T.L., Baker, M.B., Taggart, J.E., Jr., and Bruggman, P.E., 1991, The Giant Crater Lava Field: Geology and geochemistry of a compositionally zoned, high-alumina basalt to basaltic andesite eruption at Medicine Lake Volcano, California: Journal of Geophysical Research, v. 96, p. 21843–21863, doi: 10.1029/91JB01901.

Draper, D.S., and Green, T.H., 1999, P-T phase relations of silicic, alkaline, aluminous liquids: New results and applications to mantle melting and metasomatism: Earth and Planetary Science Letters, v. 170, p. 255–268, doi: 10.1016/S0012-821X(99)00111-9.

Draper, D.S., and Johnston, A.D., 1992, Anhydrous PT phase relations of an Aleutian high-MgO basalt; an investigation of the role of olivine-liquid reaction in the generation of arc high-alumina basalts: Contributions to Mineralogy and Petrology, v. 112, p. 501–519, doi: 10.1007/BF00310781.

Ducea, M.N., and Saleeby, J.B., 1996, Buoyancy sources for a large, unrooted mountain range, the Sierra Nevada, California, evidence from xenolith thermobarometry: Journal of Geophysical Research, v. 101, p. 8229–8244, doi: 10.1029/95JB03452.

Ducea, M., and Saleeby, J., 1998a, A case for delamination of the deep batholithic crust beneath the Sierra Nevada, California: International Geology Review, v. 40, p. 78–93, doi: 10.1080/00206819809465199.

Ducea, M., and Saleeby, J., 1998b, Crustal recycling beneath continental arcs: Silica-rich glass inclusions in ultramafic xenoliths from the Sierra Nevada, California: Earth and Planetary Science Letters, v. 156, p. 101–116, doi: 10.1016/S0012-821X(98)00021-1.

Dunn, T., and Sen, C., 1994, Mineral/matrix partition coefficient for orthopyroxene, plagioclase, and olivine in basaltic to andesitic systems: A combined analytical and experimental study: Geochimica et Cosmochimica Acta, v. 58, p. 717–733, doi: 10.1016/0016-7037(94)90501-0.

Elkins, L.T., Fernandes, V.A., Delano, J.W., and Grove, T.L., 2000, Origin of lunar ultramafic green glasses: Constraints from phase equilibrium studies: Geochimica et Cosmochimica Acta, v. 64, p. 2339–2350, doi: 10.1016/S0016-7037(00)00365-3.

Elkins-Tanton, L.T., and Grove, T.L., 2003, Evidence for deep melting of hydrous metasomatized mantle: Pliocene high-potassium magmas from the Sierra Nevadas: Journal of Geophysical Research, v. 108, 2350, doi: 10.1029/2002JB002168.

Elkins-Tanton, L.T., Chatterjee, N., and Grove, T.L., 2003, Experimental and petrological constraints on lunar differentiation from the Apollo 15 green picritic glasses: Meteoritics & Planetary Science, v. 38, p. 515–527, doi: 10.1111/j.1945-5100.2003.tb00024.x.

Falloon, T.J., and Danyushevsky, L.V., 2000, Melting of refractory mantle at 1.5, 2 and 2.5 GPa under anhydrous and H_2O-undersaturated conditions: Implications for the petrogenesis of high-Ca boninites and the influence of subduction components on mantle melting: Journal of Petrology, v. 41, p. 257–283, doi: 10.1093/petrology/41.2.257.

Falloon, T.J., Green, D.H., Danyushevsky, L.V., and Faul, U.H., 1999, Peridotite melting at 1.0 and 1.5 GPa: An experimental evaluation of techniques using diamond aggregates and mineral mixes for determination of near-solidus melts: Journal of Petrology, v. 40, p. 1343–1375, doi: 10.1093/petrology/40.9.1343.

Falloon, T.J., Green, D.H., O'Neill, H.S., and Hibberson, W.O., 1997, Experimental tests of low degree peridotite partial melt compositions; implications for the nature of anhydrous near-solidus peridotite melts at 1 GPa: Earth and Planetary Science Letters, v. 152, p. 149–162, doi: 10.1016/S0012-821X(97)00155-6.

Falloon, T.J., Danyushevsky, L.V., and Green, D.H., 2001, Peridotite melting at 1 GPa reversal experiments on partial melt compositions produced by peridotite-basalt sandwich experiments: Journal of Petrology, v. 42, p. 2363–2390, doi: 10.1093/petrology/42.12.2363.

Farmer, G.L., Glazner, A.F., and Manley, C.R., 2002, Did lithospheric delamination trigger late Cenozoic potassic volcanism in the southern Sierra Nevada, California?: Geological Society of America Bulletin, v. 114, p. 754–768, doi: 10.1130/0016-7606(2002)114<0754:DLDTLC>2.0.CO;2.

Feig, S.T., Koepke, J., and Snow, J.E., 2006, Effect of water on tholeiitic basalt phase equilibria: An experimental study under oxidizing conditions: Contributions to Mineralogy and Petrology, v. 152, p. 611–638, doi: 10.1007/s00410-006-0123-2.

Feldstein, S.N., and Lange, R.A., 1999, Pliocene potassic magmas from the Kings River region, Sierra Nevada,

California: Evidence of melting of a subduction-modified mantle: Journal of Petrology, v. 40, p. 1301–1320, doi: 10.1093/petrology/40.8.1301.

Fitton, J.G., James, D., and Leeman, W.P., 1991, Basic magmatism associated with late Cenozoic extension in the western United States: Compositional variations in space and time: Journal of Geophysical Research, v. 96, p. 13693–13711, doi: 10.1029/91JB00372.

Fliedner, M.M., and Ruppert, S., 1996, Three-dimensional crustal structure of the southern Sierra Nevada from seismic fan profiles and gravity modeling: Geology, v. 24, p. 367–370, doi: 10.1130/0091-7613(1996)024<0367:TDCSOT>2.3.CO;2.

Fram, M.S., and Longhi, J., 1992, Phase equilibria of dikes associated with Proterozoic anorthosite complexes: American Mineralogist, v. 77, p. 605–616.

Frassetto, A., Zandt, G., Gilbert, H., Owens, T.J., and Jones, C.H., 2011, The structure of the Sierra Nevada from receiver functions and implications for lithospheric foundering: Geosphere, v. 7, p. 898–921, doi: 10.1130/GES00570.1.

Gaetani, G.A., and Grove, T., 1998, The influence of melting of mantle peridotite: Contributions to Mineralogy and Petrology, v. 131, p. 323–346, doi: 10.1007/s004100050396.

Gaetani, G.A., Kent, A.J.R., Grove, T.L., Hutcheon, I.D., and Stolper, E.M., 2003, Mineral/melt partitioning of trace elements during hydrous peridotite partial melting: Contributions to Mineralogy and Petrology, v. 145, p. 391–405, doi: 10.1007/s00410-003-0447-0.

Garcia, M.O., Hulsebosch, T.P., and Rhodes, J.M., 1995, Olivine-rich submarine basalts from the southwest rift zone of Mauna Loa volcano: Implications for magmatic processes and geochemical evolution, *in* Rhodes, J.M., and Lockwood, J.P., eds., Mauna Loa revealed: Structure, composition, history, and hazards: American Geophysical Union Geophysical Monograph 92, p. 219–240.

Gast, P.W., 1968, Trace element fractionation and the origin of tholeiitic and alkaline magma types: Geochimica et Cosmochimica Acta, v. 32, p. 1057–1086, doi: 10.1016/0016-7037(68)90108-7.

Glazner, A.F., and Supplee, J.A., 1982, Migration of Tertiary volcanism in the southwestern United States and subduction of the Mendocino fracture zone: Earth and Planetary Science Letters, v. 60, p. 429–436, doi: 10.1016/0012-821X(82)90078-4.

Grove, T.L., and Juster, T.C., 1989, Experimental investigations of low-Ca pyroxene stability and olivine-pyroxene-liquid equilibria at 1 atm in natural basaltic and andesitic liquids: Contributions to Mineralogy and Petrology, v. 103, p. 287–305, doi: 10.1007/BF00402916.

Grove, T.L., Gerlach, D.C., and Sando, T.W., 1982, Origin of calc-alkaline series lavas at Medicine Lake Volcano by fractionation, assimilation and mixing: Contributions to Mineralogy and Petrology, v. 80, p. 160–182, doi: 10.1007/BF00374893.

Grove, T.L., Kinzler, R.J., Baker, M.B., and Donnelly-Nolan, J.M., 1988, Assimilation of granitic by basaltic magma at Burnt Lava Flow, Medicine Lake volcano, northern California: Decoupling of heat and mass transfer: Contributions to Mineralogy and Petrology, v. 99, p. 320–343, doi: 10.1007/BF00375365.

Grove, T.L., Elkins-Tanton, L.T., Parman, S.W., Chatterjee, N., Müntener, O., and Gaetani, G.A., 2003, Fractional crystallization and mantle-melting controls on calk-alkaline differentiation trends: Contributions to Mineralogy and Petrology, v. 145, p. 515–533, doi: 10.1007/s00410-003-0448-z.

Groves, K.R., 1996, Geochemical and isotopic analysis of Pleistocene basalts from the southern Coso volcanic field, California [Ph.D. thesis]: Chapel Hill, University of North Carolina, 84 p.

Hagan, J.C., Busby, C.J., Putirka, K., and Renne, P.R., 2009, Cenozoic paleocanyon evolution, ancestral Cascades arc volcanism and structure of the Hope Valley–Carson Pass region, Sierra Nevada, California: International Geology Review, v. 51, p. 777–823, doi: 10.1080/00206810903028102.

Hammond, W.C., and Humphreys, E.D., 2000, Upper mantle seismic wave velocity: Effects of realistic partial melt geometries: Journal of Geophysical Research, v. 105, p. 10975–10986, doi: 10.1029/2000JB900041.

Hays, M.R., 2004, Intra-transform volcanism along the Siqueiros Fracture Zone 8°20′N–8°30′N, East Pacific Rise [Ph.D. thesis]: Gainesville, University of Florida, 251 p.

Hedge, C.E., and Noble, D.C., 1971, Upper Cenozoic basalts with high Sr^{87}/Sr^{86} and Sr/Rb ratios, southern Great Basin, western United States: Geological Society of America Bulletin, v. 82, p. 3503–3510, doi: 10.1130/0016-7606(1971)82[3503:UCBWHS]2.0.CO;2.

Hesse, M., and Grove, T.L., 2003, Absarokites from the western Mexican Volcanic Belt: Constraints on mantle wedge conditions: Contributions to Mineralogy and Petrology, v. 146, p. 10–27, doi: 10.1007/s00410-003-0489-3.

Hoffine, S.R., 1993, Geochemistry of the volcanic rocks of the Saline Range, California: Implications for mantle composition and involvement in extension beneath the Basin and Range [Ph.D. thesis]: Lawrence, University of Kansas, 196 p.

Holbig, E.S., and Grove, T.L., 2008, Mantle melting beneath the Tibetan Plateau: Experimental constraints on ultrapotassic magmatism: Journal of Geophysical Research, v. 113, B04210, doi: 10.1029/2007JB005149.

Humphreys, E., Hessler, E., Dueker, K., Farmer, G.L., Erslev, E., and Atwater, T., 2003, How Laramide-age hydration of North American lithosphere by the Farallon slab controlled subsequent activity in the western United States: International Geology Review, v. 45, p. 575–595, doi: 10.2747/0020-6814.45.7.575.

Ito, T., and Simons, M., 2011, Temperature, and elastic moduli below the western United States: Science, v. 332, p. 947–951, doi: 10.1126/science.1202584.

Jennings, C.W., 1977, Geologic map of California: California Division of Mines and Geology, Geologic Data Map No. 2, scale 1:750,000.

Jones, C.H., Farmer, G.L., and Unruh, J., 2004, Tectonics of Pliocene removal of lithosphere of the Sierra Nevada, California: Geological Society of America Bulletin, v. 116, p. 1408–1422, doi: 10.1130/B25397.1.

Juster, T.C., Grove, T.L., and Perfit, M.R., 1989, Experimental constraints on the generation of FeTi basalts, andesite, and rhyodacites at the Galapagos spreading center, 85°W and 95°W: Journal of Geophysical Research, v. 94, p. 9251–9274, doi: 10.1029/JB094iB07p09251.

Kawamoto, T., Hervig, R.L., and Holloway, J.R., 1996, Experimental evidence for a hydrous transition zone in the early Earth's mantle: Earth and Planetary Science Letters, v. 142, p. 587–592, doi: 10.1016/0012-821X(96)00113-6.

Kelemen, P.B., Joyce, D.B., Webster, J.D., and Holloway, J.R., 1990, Reaction between ultramafic rock and fractionating basaltic magma II. Experimental investigation of reaction between olivine tholeiite and harzburgite at 1150–1050°C and 5kb: Journal of Petrology, v. 31, p. 99–134, doi: 10.1093/petrology/31.1.99.

Kinzler, R.J., 1997, Melting of mantle peridotite at pressures approaching the spinel to garnet transition: Application to mid-ocean ridge basalt petrogenesis: Journal of Geophysical Research, v. 102, p. 853–874, doi: 10.1029/96JB00988.

Kinzler, R.J., and Grove, T.L., 1992, Primary magmas of mid-ocean ridge basalts 1. Experiments and methods: Journal of Geophysical Research, v. 97, p. 6885–6906, doi: 10.1029/91JB02840.

Kistler, R.W., 1974, Phanerozoic batholiths in western North America: A summary of some recent work on variations in time, space, chemistry, and isotopic compositions: Annual Review of Earth and Planetary Sciences, v. 2, p. 403–418, doi: 10.1146/annurev.ea.02.050174.002155.

Kistler, R.W., 1990, Two different lithosphere types in the Sierra Nevada, California, *in* Anderson, J.L., ed., The nature and origin of Cordilleran magmatism: Geological Society of America Memoir 174, p. 271–281.

Kistler, R.W., and Peterman, Z.E., 1973, Variations in Sr, Rb, K, Na, and Initial Sr^{87}/Sr^{86} in Mesozoic granitic wall rocks and intruded wall rocks in central California: Geological Society of America Bulletin, v. 84, p. 3489–3512, doi: 10.1130/0016-7606(1973)84<3489:VISRKN>2.0.CO;2.

Koerner, A., Busby, C., Putirka, K., and Pluhar, C.J., 2009, New evidence for alternative effusion and explosive eruptions from the type section of the Stanislaus Group in the "Cataract" paleocanyon, central Sierra Nevada: International Geology Review, v. 51, doi: 10.1080/00206810903028185.

Kylander-Clark, A.R.C., Coleman, D.S., Glazner, A.F., and Bartley, J.M., 2005, Evidence for 65 km of dextral slip across the Owens Valley, California, since 83 Ma: Geological Society of America Bulletin, v. 117, p. 962–968, doi: 10.1130/B25624.1.

Lackey, J.S., Valley, J.W., Chen, J.H., and Stockli, D.F., 2008, Dynamic magma systems, crustal recycling, and alteration in the central Sierra Nevada batholith: The oxygen isotope record: Journal off: Petrology, v. 49, p. 1397–1426, doi: 10.1093/petrology/egn030.

Lange, R.A., and Carmichael, I.S.E., 1996, The Aurora volcanic field, California-Nevada: Oxygen fugacity constrains on the development of andesitic magma: Contributions to Mineralogy and Petrology, v. 125, p. 167–185, doi: 10.1007/s004100050214.

LaPorte, D., Toplis, M.J., Seyler, M., and Devidal, J.-L., 2004, A new experimental technique for extracting liquids from peridotite at very low degrees of melting: Application to partial melting of depleted peridotite: Contributions to Mineralogy and Petrology, v. 146, p. 463–484, doi: 10.1007/s00410-003-0509-3.

Lee, C.T.A., 2005, Trace element evidence for hydrous metasomatism at the base of the North American lithosphere and possible association with Laramide low-angle subduction: Journal of Geology, v. 113, p. 673–685, doi: 10.1086/449327.

Lee, C.T., Rudnick, R.L., and Brimhall, G.H., 2001, Deep lithospheric dynamics beneath the Sierra Nevada during the Mesozoic and Cenozoic as inferred from xenolith petrology: Geochemistry, Geophysics, Geosystems, v. 2, 2001GC000152, 27 p.

Lee, C.T.A., Cheng, X., and Horodyskyj, U., 2006, The development and refinement of continental arcs by primary basaltic magmatism, garnet pyroxenite accumulation, basaltic recharge and delamination: insights form the Sierra Nevada, California: Contributions to Mineralogy and Petrology, v. 151, p. 222–242, doi: 10.1007/s00410-005-0056-1.

Lee, C.T.A., Luffi, P., Plank, T., Dalton, H., and Leeman, W.P., 2009, Constraints on the depths and temperatures of basaltic magma generation on Earth and other terrestrial planets using new thermobarometers for mafic magmas: Earth and Planetary Science Letters, v. 279, p. 20–33, doi: 10.1016/j.epsl.2008.12.020.

Leeman, W.P., 1970, The isotopic composition of strontium in late Cenozoic basalts from the Basin-Range province, western United States: Geochimica et Cosmochimica Acta, v. 34, p. 857–872, doi: 10.1016/0016-7037(70)90124-9.

Leeman, W.P., 1974, Late Cenozoic alkali-rich basalt from the western Grand Canyon area, Utah and Arizona: Isotopic composition of strontium: Geological Society of America Bulletin, v. 85, p. 1691–1696, doi: 10.1130/0016-7606(1974)85<1691:LCABFT>2.0.CO;2.

Leeman, W.P., and Harry, D.L., 1993, A binary source for extension-related magmatism in the Great Basin, western North America: Science, v. 262, p. 1550–1554, doi: 10.1126/science.262.5139.1550.

Leeman, W.P., Lewis, J.F., Evarts, R.C., Contrey, R.M., and Streck, M.J., 2005, Petrologic constraints on the thermal structure of the Cascades arc: Journal of Volcanology and Geothermal Research, v. 140, p. 67–105, doi: 10.1016/j.jvolgeores.2004.07.016.

Le Pourhiet, L., Gurnis, M., and Saleeby, J., 2006, Mantle instability beneath the Sierra Nevada Mountains in California and Death Valley extension: Earth and Planetary Science Letters, v. 251, p. 104–119, doi: 10.1016/j.epsl.2006.08.028.

Li, X., Yuan, X., and Kind, R., 2007, The lithosphere-asthenosphere boundary beneath the western United States: Geophysical Journal International, v. 170, p. 700–710, doi: 10.1111/j.1365-246X.2007.03428.x.

Lister, J.R., and Kerr, R.C., 1991, Fluid-mechanical models of crack propagation and their application to magma transport in dykes: Journal of Geophysical Research, v. 96, p. 10049–10077, doi: 10.1029/91JB00600.

Longhi, J., 1995, Liquidus equilibria of some primary lunar and terrestrial melts in the garnet stability field:

Geochimica et Cosmochimica Acta, v. 59, p. 2375–2386, doi: 10.1016/0016-7037(95)00111-C.

Longhi, J., and Pan, V., 1988, A reconnaissance study of phase boundaries in low-alkali basaltic liquids: Journal of Petrology, v. 29, p. 115–147, doi: 10.1093/petrology/29.1.115.

Luhr, J.F., and Carmichael, I.S.E., 1980, The Colima volcanic complex, Mexico. I: Post-caldera andesites from Volcan Colima: Contributions to Mineralogy and Petrology, v. 71, p. 343–372, doi: 10.1007/BF00374707.

Lum, C.C.L., Leeman, W.P., Foland, K.A., Kargel, J.A., and Fitton, J.G., 1989, Isotopic variations in continental basaltic lavas as indicators of mantle heterogeneity: Examples from the western U.S. Cordillera: Journal of Geophysical Research, v. 94, p. 7871–7884, doi: 10.1029/JB094iB06p07871.

Maaloe, S., 2004, The PT-phase relations of an MgO-rich Hawaiian tholeiite: The compositions of primary Hawaiian tholeiites: Contributions to Mineralogy and Petrology, v. 148, p. 236–246, doi: 10.1007/s00410-004-0601-3.

MacDonald, R., Smith, R.L., Robert, L., and Thomas, J.E., 1992, Chemistry of the subalkalic silicic obsidians: U.S. Geological Survey Professional Paper P-1523, 214 p.

McDade, P., Blundy, J.D., and Wood, B.J., 2003, Trace element partitioning on the Tinaquillo lherzolite solidus at 1.5 GPa: Physics of the Earth and Planetary Interiors, v. 139, p. 129–147, doi: 10.1016/S0031-9201(03)00149-3.

McQuarrie, N., and Wernicke, B.P., 2005, An animated tectonic reconstruction of southwestern North America since 36 Ma: Geosphere, v. 1, p. 147–172, doi: 10.1130/GES00016.1.

Meen, J.K., 1990, Elevation of potassium content of basaltic magma by fractional crystallization: The effect of pressure: Contributions to Mineralogy and Petrology, v. 104, p. 309–331, doi: 10.1007/BF00321487.

Moore, J.G., and Doge, F.C.W., 1980, Late Cenozoic volcanic rocks of the southern Sierra Nevada, California: I. Geology and petrology: Summary: Geological Society of America Bulletin, v. 91, p. 515–518, doi: 10.1130/0016-7606(1980)91<515:LCVROT>2.0.CO;2.

Mordick, B.E., and Glazner, A.F., 2006, Clinopyroxene thermobarometry of basalts from the Coso and Big Pine volcanic fields, California: Contributions to Mineralogy and Petrology, v. 152, p. 111–124, doi: 10.1007/s00410-006-0097-0.

Mukhopadhyay, B., and Manton, W.I., 1994, Upper-mantle fragments from beneath the Sierra Nevada batholith: Partial fusion, fractional crystallization, and metasomatism in a subduction-related ancient lithosphere: Journal of Petrology, v. 35, p. 1414–1450, doi: 10.1093/petrology/35.5.1417.

Muffler, L., Blakely, R., and Clynne, M., 2008, Interaction of the Walker Lane and the Cascade Volcanic Arc, northern California: American Geophysical Union, Fall meeting, abs. T23B–2032.

Müntener, O., Kelemen, P.B., and Grove, T.L., 2001, The role of H_2O during crystallization of primitive arc magmas under uppermost mantle conditions and genesis of igneous pyroxenites: An experimental study: Contributions to Mineralogy and Petrology, v. 141, p. 643–658, doi: 10.1007/s004100100266.

Mussel White, D.S., Dalton, H.A., Kiefer, W.S., and Treiman, A.H., 2006, Experimental petrology of the basaltic shergottite Yamato-980459: Implications for the thermal structure of the Martian mantle: Meteoritics & Planetary Science, v. 41, p. 1271–1290, doi: 10.1111/j.1945-5100.2006.tb00521.x.

Nicholls, J., Carmichael, I.S.E., and Stormer, J.C., 1971, Silica activity and P_{total} in igneous rocks: Contributions to Mineralogy and Petrology, v. 33, p. 1–20, doi: 10.1007/BF00373791.

Ormerod, D.S., 1988, Late- to post-subduction magmatic transition in the western Great Basin, U.S.A. [Ph.D. thesis]: Open University, UK, 331 p.

Ormerod, D.S., Hawkesworth, C.J., Rogers, N.W., Leeman, W.P., and Menzies, M.A., 1988, Tectonic and magmatic transitions in the western Great Basin, USA: Nature, v. 333, p. 349–353, doi: 10.1038/333349a0.

Ormerod, D.S., Rogers, N.W., and Hawkesworth, C.J., 1991, Melting in the lithospheric mantle: Inverse modelling of alkali-olivine basalts form the Big Pine Volcanic Field, California: Contributions to Mineralogy and Petrology, v. 108, p. 305–317, doi: 10.1007/BF00285939.

Parman, S.W., and Grove, T.L., 2004, Harzburgite melting with and without H_2O: Experimental data and predictive modeling: Journal of Geophysical Research, v. 109, doi: 10.1029/2003JB002566.

Parman, S.W., Dann, J.C., Grove, T.L., and deWit, M.J., 1997, Emplacement conditions of komatiite magmas from the 3.49 Ga Komati Formation, Barberton Greenstone Belt, South Africa: Earth and Planetary Science Letters, v. 150, p. 303–323, doi: 10.1016/S0012-821X(97)00104-0.

Pichavant, M., Mysen, B.O., and MacDonald, R., 2002, Source and H_2O content of high-MgO magmas in island arc settings: An experimental study of a primitive calc-alkaline basalt from St. Vincent, Lesser Antilles arc: Geochimica et Cosmochimica Acta, v. 66, p. 2193–2209, doi: 10.1016/S0016-7037(01)00891-2.

Pickering-Witter, J., and Johnston, A.D., 2000, The effects of variable bulk composition on the melting systematics of fertile peridotitic assemblages: Contributions to Mineralogy and Petrology, v. 140, p. 190–211, doi: 10.1007/s004100000183.

Plank, T., 2005, Constraints from thorium/lanthanum on sediment recycling at subduction zones and the evolution of the continents: Journal of Petrology, v. 46, p. 921–944, doi: 10.1093/petrology/egi005.

Powers, H.A., 1955, Composition and origin of basaltic magma of the Hawaiian Islands: Geochimica et Cosmochimica Acta, v. 7, p. 77–107, doi: 10.1016/0016-7037(55)90047-8.

Putirka, K.D., 2008, Thermometers and barometers for volcanic systems, *in* Putirka, K.D., and Tepley, F., eds., Minerals, inclusions and volcanic processes: Mineralogical Society of America Reviews in Mineralogy and Geochemistry Volume 69, p. 61–120, doi: 10.2138/rmg.2008.69.3.

Putirka, K., and Busby, C.J., 2007, The tectonic significance of high K_2O volcanism in the Sierra Nevada, California: Geology, v. 35, p. 923–926, doi: 10.1130/G23914A.1.

Putirka, K., and Condit, C., 2003, A cross section of a magma conduit system at the margins of the Colorado Plateau: Geology, v. 31, p. 701–704, doi: 10.1130/G19550.1.

Putirka, K., Ryerson, F.J., and Mikaelian, H., 2003, New igneous thermobarometers for mafic and evolved lava compositions, based on clinopyroxene + liquid equilibria: American Mineralogist, v. 88, p. 1542–1554.

Putirka, K., Perfit, M., Ryerson, F.J., and Jackson, M.G., 2007, Ambient and excess mantle temperatures, olivine thermometry, and active vs. passive upwelling: Chemical Geology, v. 241, p. 177–206, doi: 10.1016/j.chemgeo.2007.01.014.

Putirka, K.D., Ryerson, F.J., Perfit, M., and Ridley, W.I., 2011, Mineralogy and composition of the oceanic mantle: Journal of Petrology, v. 52, p. 279–313, doi: 10.1093/petrology/egq080.

Ramo, O.T., Caliza, J.P., and Kosunen, P.J., 2002, Geochemistry of Mesozoic plutons, southern Death Valley region, California; insights into the origin of Cordilleran interior magmatism: Contributions to Mineralogy and Petrology, v. 143, p. 416–437, doi: 10.1007/s00410-002-0354-9.

Ransome, F.L., 1898, Some lava flows of the western slope of the Sierra Nevada, California: American Journal of Science, v. 5, p. 355–375, doi: 10.2475/ajs.s4-5.29.355.

Ratajeski, K., Sisson, T.W., and Glazner, A.F., 2005, Experimental and geochemical evidence for derivation of the El Capitan Granite, California, by partial melting of hydrous gabbroic lower crust: Contributions to Mineralogy and Petrology, v. 149, p. 713–734, doi: 10.1007/s00410-005-0677-4.

Rayleigh, J.W.S., 1896, Theoretical considerations respecting the separation of gases by diffusion and similar processes: Philosophical Magazine, v. 42, p. 493–498.

Righter, K., and Carmichael, I.S.E., 1996, Phase equilibria of phlogopite lamprophyres from western Mexico: Biotite-liquid equilibria and P-T estimates for biotite-bearing igneous rocks: Contributions to Mineralogy and Petrology, v. 123, p. 1–21, doi: 10.1007/s004100050140.

Robinson, J.A.C., Wood, B.J., and Blundy, J.D., 1998, The beginning of melting of fertile and depleted peridotite at 1.5 GPa: Earth and Planetary Science Letters, v. 155, p. 97–111, doi: 10.1016/S0012-821X(97)00162-3.

Rogers, N.W., Hawkesworth, C.J., and Ormerod, D.S., 1995, Late Cenozoic basaltic magmatism in the Western Great Basin, California and Nevada: Journal of Geophysical Research, v. 100, p. 10287–10301, doi: 10.1029/94JB02738.

Roullet, F., 2006, The late Miocene Dixie Mountain Volcanic Center, northern Sierra Nevada: Eroded stratovolcano or laccolithic intrusion? [M.S. thesis]: Santa Barbara, University of California, 128 p.

Saleeby, J.B., Sams, D.B., and Kistler, R.W., 1987, U/Pb zircon, strontium, and oxygen isotopic and geochronologic study of the southernmost Sierra Nevada batholith, California: Journal of Geophysical Research, v. 92, p. 10443–10466, doi: 10.1029/JB092iB10p10443.

Salters, V.J.M., and Longhi, J., 1999, Trace element partitioning during the initial stages of melting beneath mid-ocean ridges: Earth and Planetary Science Letters, v. 166, p. 15–30, doi: 10.1016/S0012-821X(98)00271-4.

Savage, B., Ji, C., and Helmberger, D.V., 2003, Velocity variations in the uppermost mantle beneath the southern Sierra Nevada and Walker Lane: Journal of Geophysical Research, v. 108, 2325, doi: 10.1029/2001JB001393.

Schmandt, B., and Humphreys, E., 2010, Seismic heterogeneity and small-scale convection in the southern California upper mantle: Geochemistry Geophysics Geosystems, v. 11, Q05004, doi: 10.1029/2010GC003042.

Schmidt, K., Bottazzi, P., Vannucci, R., and Mengel, K., 1999, Trace element partitioning between phlogopite, clinopyroxene, and leucite lamproite melt: Earth and Planetary Science Letters, v. 168, p. 287–299, doi: 10.1016/S0012-821X(99)00056-4.

Schwab, B.E., and Johnston, A.D., 2001, Melting systematics of modally variable, compositionally intermediate peridotites and the effects of mineral fertility: Journal of Petrology, v. 42, p. 1789–1811, doi: 10.1093/petrology/42.10.1789.

Snow, J.K., and Wernicke, B.P., 2000, Cenozoic tectonism in the central Basin and Range: Magnitude, rate, and distribution of upper crustal strain: American Journal of Science, v. 300, p. 659–719, doi: 10.2475/ajs.300.9.659.

Stewart, J.H., and Carlson, J.E., 1977, Preliminary geologic map of Nevada: Nevada Bureau of Mines and Geology, Map 57, scale 1:1,000,000.

Stolper, E., 1980, A phase diagram for mid-ocean ridge basalts: Preliminary results and implications for petrogenesis: Contributions to Mineralogy and Petrology, v. 74, p. 13–27, doi: 10.1007/BF00375485.

Takada, A., 1994, The influence of regional stress and magmatic input on styles of monogenetic and polygenetic volcanism: Journal of Geophysical Research, v. 99, p. 13563–13573, doi: 10.1029/94JB00494.

Takagi, D., Sato, H., and Nakagawa, N., 2005, Experimental study of a low-alkali tholeiite at 1–5 kbar: Optimal condition for the crystallization of high-An plagioclase in hydrous arc tholeiite: Contributions to Mineralogy and Petrology, v. 149, p. 527–540, doi: 10.1007/s00410-005-0666-7.

Takahashi, E., 1980, Melting relations of an alkali-olivine basalt to 30 kbar, and their bearing on the origin of alkali basalt magmas: Carnegie Institute of Washington Year Book, v. 79, p. 271–276.

Till, C., Elkins-Tanton, L.T., and Fischer, K.M., 2010, A mechanism for low-extent melts at the lithosphere-asthenosphere boundary: Geochemistry Geophysics Geosystems, v. 11, Q10015, doi: 10.1029/2010gc003234.

Vander Auwera, J., Longhi, J., and Duchesne, J.-C., 1998, A liquid line of descent of the jotunite (hypersthene monzodiorite) suite: Journal of Petrology, v. 39, p. 439–468, doi: 10.1093/petrology/39.3.439.

Van Kooten, G.K., 1980, Mineralogy, petrology, and geochemistry of an ultrapotassic basaltic suite, central Sierra Nevada, California, USA: Journal of Petrology, v. 21, p. 651–684, doi: 10.1093/petrology/21.4.651.

Villiger, S., Ulmer, P., Muntener, O., and Thompson, A.B., 2004, The liquid line of descent of anhydrous, mantle-derived, tholeiitic liquids by fractional and equilibrium crystallization—An experimental study at 1.0 GPa: Journal of Geology, v. 45, p. 2369–2388, doi: 10.1093/petrology/egh042.

Wagner, T.P., and Grove, T.L., 1998, Melt/harzburgite reaction in the petrogenesis of tholeiitic magma from Kilauea volcano, Hawaii: Contributions to Mineralogy and Petrology, v. 131, p. 1–12, doi: 10.1007/s004100050374.

Waits, J.R., 1995, Geochemical and isotopic study of peridotite-bearing lavas in eastern California [M.S. thesis]: Chapel Hill, University of North Carolina, 118 p.

Wakabayashi, J., and Sawyer, T.L., 2001, Stream incision, tectonics, uplift, and evolution of topography of the Sierra Nevada, California: Journal of Geology, v. 109, p. 539–562, doi: 10.1086/321962.

Walker, J.D., and Coleman, D.S., 1991, Geochemical constraints on mode of extension in the Death Valley region: Geology, v. 19, p. 971–974, doi: 10.1130/0091-7613(1991)019<0971:GCOMOE>2.3.CO;2.

Walter, M.J., 1998, Melting of garnet peridotite and the origin of komatiite and depleted lithosphere: Journal of Petrology, v. 39, p. 29–60, doi: 10.1093/petrology/39.1.29.

Wang, K., Plank, T., Walker, J.D., and Smith, E.I., 2002, A mantle melting profile across the Basin and Range, SW USA: Journal of Geophysical Research, v. 107, 2017, doi: 10.1029/2001JB000209.

Wasylenki, L.E., Baker, M.B., Kent, A.J.R., and Stolper, E.M., 2003, Near-solidus melting of the shallow upper mantle: Partial melting experiments on depleted peridotite: Journal of Petrology, v. 44, p. 1163–1191, doi: 10.1093/petrology/44.7.1163.

Wernicke, B., and 18 others, 1996, Origin of high mountains in the continents: The southern Sierra Nevada: Science, v. 271, p. 190–193, doi: 10.1126/science.271.5246.190.

Workman, R.K., and Hart, S.R., 2005, Major and trace element composition of the depleted MORB mantle (DMM): Earth and Planetary Science Letters, v. 231, p. 53–72, doi: 10.1016/j.epsl.2004.12.005.

Wright, T.L., and Fiske, R.S., 1971, Origin of the differentiated and hybrid lavas of Kilauea volcano, Hawaii: Journal of Petrology, v. 12, p. 1–65, doi: 10.1093/petrology/12.1.1.

Xirouchakis, D., Hirschmann, M.M., and Simpson, J., 2001, The effect of titanium on the silica content and on mineral-liquid partitioning of mantle-derived melts: Geochimica et Cosmochimica Acta, v. 65, p. 2201–2217, doi: 10.1016/S0016-7037(00)00549-4.

Zandt, G., Gilbert, H., Owens, T.J., Ducea, M., Saleeby, J., and Jones, C.H., 2004, Active foundering of a continental arc root beneath the southern Sierra Nevada in California: Nature, v. 431, p. 41–46, doi: 10.1038/nature02847.

Manuscript Received 10 June 2011
Revised Manuscript Received 22 November 2011
Manuscript Accepted 25 November 2011